

## Assessment and evolution analysis of the global wood pulp trade network resilience based on underload cascading failure

Wujun Tian <sup>a</sup>, Xiangyu Huang <sup>b,c</sup>, Liuguo Shao <sup>d,e</sup>, Zhongwei Wang <sup>b,c</sup>, Yihua Li <sup>b,c</sup>

<sup>a</sup> Central South University of Forestry and Technology, College of Computer Science and Mathematics, 410004, China

<sup>b</sup> Central South University of Forestry and Technology, College of logistics, 410004, China

<sup>c</sup> Central South University of Forestry and Technology, College of economics and management, 410004, China

<sup>d</sup> Central South University, Business School, Changsha 410083, China

<sup>e</sup> Central South University, Institute of Metal Resources Strategy, Changsha 410083, China

### ARTICLE INFO

Handling Editor: Yutao Wang

Dataset link: <https://comtradeplus.un.org>

**Keywords:**

Pulp trade network  
Complex network modeling  
Resilience assessment  
Cascading failure model  
Sustainable forest management

### ABSTRACT

This study aims to assess the resilience of the global pulp trade network by applying complex network modeling methods. A directed weighted network model was constructed based on UN commodity trade data from 2002 to 2023, and a dynamic resilience evaluation framework based on an underload cascading failure model was proposed, systematically revealing both static and dynamic resilience characteristics during the network's spatiotemporal evolution. Findings show that the global pulp trade network exhibits significant spatiotemporal evolution: while the number of nodes has decreased, the number of edges continues to increase, reinforcing the dominance of core countries such as China and Brazil. The multipolar trend has led to the formation of five major communities. Although total trade volume remains stable — reflecting the industrial necessity of pulp — different external shocks have distinct impacts: the financial crisis triggered delayed effects through market adjustments, whereas the outbreak of the pandemic initiated immediate institutional interventions. Static resilience analysis reveals significantly improved network transmission efficiency, with high-trade-volume countries becoming less clustered. Assortativity patterns indicate continued dependency of smaller countries on central nodes, while power-law fitting suggests weakened hierarchy and increased robustness against targeted attacks due to diversified structures. Notably, China's role as a hub has grown rapidly, with its incoming strength increasing by 5.14 times and weighted betweenness centrality rising by 3.54 times. Cascading failure simulation further demonstrates that the failure of key nodes, such as Brazil, may trigger large-scale chain reactions, directly causing trade reductions in 32 countries. Under targeted attack scenarios, network performance loss far exceeds random disruptions, confirming the structural risks associated with supply concentration. Dynamic resilience optimization shows that reducing failure thresholds can enhance global efficiency redundancy by 5.57 times and increase the strength of the largest connected subgraph by 3.59 times, offering quantitative support for resilience-enhancing strategies. Moreover, external shocks exhibit two distinct modes of impact on network resilience: the financial crisis induced gradual adaptation via market mechanisms, while the pandemic triggered emergency response mechanisms, highlighting the critical role of institutional intervention in supply chain stability and revealing fundamental differences between market-driven and policy-driven resilience pathways. The innovations of this research lie in the first application of an underload cascading failure model to pulp trade network resilience assessment, breaking through the limitations of traditional static analyses. It also constructs a dynamic resilience evaluation framework integrated with this model, enabling end-to-end analysis from failure simulation to resilience quantification. By transforming time-series responses into quantifiable metrics through cumulative integration, this work addresses the lack of standardized resilience indicators in forest product trade networks. The findings provide scientific support for policies related to supply chain security, sustainable forest management, and cleaner production practices.

\* Corresponding authors.

E-mail addresses: [20223523@csuft.edu.cn](mailto:20223523@csuft.edu.cn) (W. Tian), [xyhuang@csuft.edu.cn](mailto:xyhuang@csuft.edu.cn) (X. Huang), [shaoliuguo@csu.edu.cn](mailto:shaoliuguo@csu.edu.cn) (L. Shao).

## 1. Introduction

Wood pulp, due to its widespread applications, sustainability, and environmental characteristics, occupies a crucial position in industries such as papermaking, textiles, and packaging (Worku et al., 2023). As an integral part of the global economy, pulp trade is vital for economic growth, the supply of papermaking raw materials, and the utilization and conservation of forest resources (Rossato et al., 2018). The pulp and paper industry is one of the most energy-intensive sectors globally (Andersson and Thollander, 2019). The distribution of global wood pulp resources is uneven, with major producers including Brazil, Canada, Russia, and the United States. Through trade, supply and demand are adjusted, contributing to economic development (Sun, 2015; de Carvalho et al., 2009). From 2002 to 2023, the global pulp trade volume increased from \$17.4 billion to \$48.5 billion, with an average annual growth rate of 8.5%, and the trade volume expanded from 41.01 million tons to 68.09 million tons, with an annual growth rate of 3.1%. The global pulp trade system is complex, with a global division of labor in production, resulting in an intertwined network structure.

Research on global wood pulp and wood product trade networks indicates that the pulp and paper industry is undergoing structural changes that significantly impact global national economies. There are significant differences in regional market shares, production capacities, and consumption patterns (Hujala et al., 2013; McCarthy and Lei, 2010). Scholars have conducted in-depth studies on the pulp import characteristics of China, a key participant in fiber trade (Sun, 2015). The COVID-19 pandemic has had a tremendous impact on global industrial supply chains, posing challenges to the pulp and paper industry while also creating opportunities for demand growth (Liu et al., 2020). As a key component of wood-based forest products, the evolution of pulp trade patterns has profound implications for the global forestry economy. Research shows that the global forest products trade network is becoming increasingly complex, with network efficiency improving, and high-GDP countries playing a dominant role. Studies have not only analyzed trade relationships but also identified core participants and explored the connections of RCEP countries in the wood product trade network (Zhou et al., 2021; Fang et al., 2021; Wang et al., 2023b; Lovric et al., 2018). Scholars analyzing the evolution of the global forest product trade network from 1995 to 2020 have found a sustained growth trend and have used disruption simulation methods to assess network resilience (Liu et al., 2024). Current research on forest product trade networks remains limited compared to other resource trade networks. Systematic analyses are notably lacking, particularly in understanding network resilience mechanisms. Recent global supply chain disruptions — including geopolitical conflicts, extreme weather events, and policy changes — have significantly impacted wood pulp supply stability. These challenges highlight the critical need to develop dedicated resilience assessment frameworks for wood pulp trade networks.

In recent years, research on the resilience of complex networks has gradually increased. The concept was originally derived from the field of mechanics to describe the ability of materials to recover to their original state after an external force impact (Holling, 1973). It was subsequently innovatively introduced into the field of ecosystem restoration and further expanded to more complex socio-ecological systems. In this context, resilience refers to the ability of individual components in a network system, through collaboration and complementarity in social, economic, and organizational domains, to withstand and adapt to acute shocks and chronic stresses and recover or transform (Li et al., 2019; Wei and Xiu, 2020). With the continuous development of complex network theory, research on network resilience has garnered increasing attention, particularly in fields such as ecological networks, economic networks, transportation networks, supply chain networks, and urban networks (Akbarzadeh et al., 2019; Kharrazi et al., 2016, 2017; Mohammed et al., 2023; Liu and Song, 2020).

Research on network resilience encompasses multiple aspects, including complex network characteristic analysis and infrastructure resilience enhancement. Gao et al. (2016) and Kim et al. (2015) emphasize the importance of network structural adjustment in enhancing resilience. Ash and Newth (2007) and Zhao et al. (2011) studied the resilience of networks in cascading failures and disruptions, providing theoretical support for structural optimization. Berche et al. (2009) and Reggiani (2013) assessed the resilience of public transportation and transport networks. Kammouh et al. (2020) and Herrera et al. (2016) proposed new tools for resilience assessment, applied to engineering systems and water supply networks. Chopra et al. (2016) and Li et al. (2020a) proposed resilience enhancement strategies for specific infrastructures. Serre and Heinzel (2018) and Azadegan and Dooley (2021) studied cascading effects in natural disasters and supply chains, proposing multi-level collaborative strategies. John et al. (2016) and Kilanitis and Sextos (2019) used Bayesian networks and comprehensive evaluation frameworks to assess the resilience of port and road networks. Gao et al. (2015a), Kim et al. (2017), Liu et al. (2022), and Wei and Xiu (2020) reviewed progress in network resilience, emphasizing dynamic complexity and interdisciplinary research. Artine et al. (2024) and Wan et al. (2021a) discussed the application of robustness, elasticity, and centrality indicators in resilience analysis. Network resilience measurement indicators can be categorized into two major dimensions: structural resilience and node resilience, as outlined in Tables 1 and 2.

As shown in Table 1, existing studies have investigated resilience metrics for complex networks through dimensions such as redundancy, connectivity, clustering, hierarchy, and assortativity. However, a systematic evaluation framework remains underdeveloped, with notable correlations and redundancies observed among certain indicators. Given the distinctive topological characteristics of the wood pulp trade network, this study prioritizes the selection of key independent indicators tailored to its structural properties to ensure assessment validity. Furthermore, establishing appropriate weightings for path-dependent resilience metrics is essential for constructing a robust analytical framework to evaluate resource trade network resilience.

As shown in Table 2, existing studies have used metrics such as K-shell and degree centrality to measure node resilience. However, these metrics exhibit overlapping correlations. Simulations indicate that closeness centrality has a weak correlation with the resilience of the wood pulp trade network, and the K-shell metric struggles to adapt to the characteristics of weighted directed networks. This study will screen key indicators with independent explanatory power based on the directed and weighted features of the wood pulp trade network to construct a precise evaluation framework.

In trade network resilience studies, the transmission mechanism of cascading failure risks is seldom addressed. However, the complex network field has made significant progress in this area, providing valuable insights. Existing cascading failure models mainly include the sandpile model, CASCADE model, OPA model, and load-capacity model, all of which assign initial load and capacity to nodes (or edges). When a node fails, the load is redistributed according to specific principles. Key influencing factors include the initial load, capacity, and load redistribution strategies of nodes (or edges) (Carreras et al., 2002; Lee et al., 2004; Moreno et al., 2001; Sansavini et al., 2009; Xia et al., 2010). Initial load studies have evolved from uniform assumptions to the use of node betweenness, then simplified to degree functions, and later redefined considering the degree of neighboring nodes (Moreno et al., 2001; Duan et al., 2013, 2014; Duo, 2010). Node capacity is categorized into three types: independent of the initial load, proportional to the initial load, and nonlinear (Holme et al., 2002; Li et al., 2008; Wang et al., 2013; Moreno et al., 2007). Load redistribution strategies serve as the final barrier to mitigating cascading failures, including average allocation, random allocation, global allocation, local preferential allocation, and adjustable load redistribution. The adjustable strategy proposed by

**Table 1**

Summary of complex network structure toughness measures and related literature.

Evaluation dimension	Measurement metrics	Selected references to literature
Redundancy	Network density	Chen and Chen (2023) and Miao et al. (2024)
	Number of node edges	Chen and Chen (2023) and Xu and Xu (2024)
Connectivity	Average degree	Kim et al. (2015)
	Global efficiency	Bai et al. (2023) and Ji et al. (2024a)
	Average path length	Herrera et al. (2016) and Zhao et al. (2011)
Clustering	Diameter	Zhao et al. (2011) and Yuan et al. (2022)
	Percentage of maximum connected subgraph nodes	Dong et al. (2021), Li et al. (2020a) and Artimo et al. (2024)
	Average number of independent paths	Li et al. (2024)
Hierarchicality	Clustering coefficient	Liu et al. (2022), Berche et al. (2009) and Li et al. (2020b)
	Modularity	Chopra et al. (2016)
	Reciprocity	Miao et al. (2024)
Matchability	Degree Distribution	Gao et al. (2015b) and Reggiani (2013)
	Gini coefficient	Sun et al. (2023)
	Pearson's correlation coefficient	Ash and Newth (2007)

**Table 2**

Summary of complex network node toughness measures and related literature.

Evaluation Dimension	Measurement metrics	Selected references to literature
Core dimensions	K-shell	Wu et al. (2024) and Wan et al. (2021b)
Local connectivity	Degree centrality	Ji et al. (2024b) and Xiang et al. (2024)
Dynamic adaptability	Eigenvector centrality	Clark et al. (2018)
Information accessibility	Proximity centrality	Wan et al. (2021b)
Information flow graphicality	Mesonometric centrality	Kim et al. (2015) and Xu and Xu (2024)
Dynamic adaptability	PageRank centrality	Meng et al. (2023)

Duan et al. offers new insights for load redistribution research (Duan et al., 2014; Li et al., 2008; Moreno et al., 2007; Duo, 2010).

In recent years, research on cascading failures in trade networks has gradually emerged. Cai and Song (2016) applied complex network theory to international agricultural trade and introduced an improved Bootstrap percolation model to simulate cascading impacts following trade relationship disruptions. Lee and Goh (2016) emphasized the critical role of cascading failures in multilayer networks, providing a new perspective for understanding the complex dynamics of international trade networks. Chen et al. (2022) developed a network dynamics model based on the improved Bootstrap percolation theory to simulate cascading diffusion in international oil trade disruptions. Recent studies on oil, cobalt, aluminum, polysilicon, and wind energy equipment trade networks (Sun et al., 2022; Zhao et al., 2023; Wang et al., 2023a; Miao et al., 2024) have analyzed network robustness and risk propagation paths using cascading failure models.

Current research on cascading failures has primarily focused on overload failures in infrastructure networks. However, failures in trade networks mainly manifest as underload failures, which differ in mechanism. Underload failures can trigger unique dynamic effects and network reconfiguration. To better understand these characteristics, it is necessary to integrate multidisciplinary approaches, including resource security, complex network theory, and network dynamics. This integration can enhance the resilience of trade networks and provide new research perspectives.

Research on trade network resilience based on complex network theory has provided a valuable foundation for this study, but there are still some research gaps. (1) The research on trade network resilience lacks systematic and widely accepted assessment standards. Given the unique nature of each network, customized resilience evaluation indicators should be devised for specific networks. (2) Currently, research on dynamic resilience assessment under disruption disturbances in trade network resilience evaluations is still in its early stages, and the impact of cascading failures has not been incorporated. Due to fundamental differences, cascading failure models for other types of networks cannot be directly applied to the assessment of trade network resilience. (3) Compared to resilience research in the resource and food trade network industries, research on forest product trade networks is relatively insufficient, and resilience research on wood pulp trade

networks remains a significant gap. This necessitates a comprehensive analysis of the evolution of wood pulp trade network resilience from both temporal and spatial dimensions. Therefore, based on the global trade data of wood pulp from the United Nations Comtrade Database spanning from 2002 to 2023, this paper first constructs a directed and weighted trade network. Subsequently, a model for underload cascading failure is developed, and empirical research is conducted on both the static resilience and dynamic structural resilience of the network.

The specific contributions are as follows: (1) A model for underload cascading failure under trade network disruption disturbances was constructed and simulated. (2) A dynamic resilience assessment method for the wood pulp trade network, considering underload cascading failure, was proposed, filling a gap in the dynamic resilience assessment indicator system for forest product trade networks. (3) A visual analysis of the static structural resilience, static node resilience, and dynamic structural resilience of the wood pulp trade network was conducted from both temporal and spatial perspectives, highlighting the importance of visualization in studying network resilience. This analysis is of great significance for enhancing the security and stability of the wood pulp trade supply. The remainder of this paper is organized as follows. Section 2 introduces the data sources, research framework, model construction, and indicator design. Section 3 presents the analysis of simulation results, followed by a conclusion in the final section.

## 2. Data sources and research methodology

### 2.1. Data sources

This study is based on data from the United Nations Comtrade Database spanning from 2002 to 2023, covering over 50,000 trade records from 165 countries and regions. To ensure data consistency, and in accordance with the World Bank's technical note on "Imports, Exports and Mirror Data with UN COMTRADE, World Bank (2024)" this study employs import statistics, which offer more standardized reporting practices. However, this approach may potentially underestimate informal trade activities. Furthermore, this study merges Hong Kong and Macao data into mainland China. Their wood pulp exports account for 43% of the combined total due to re-export advantages, while

**Table 3**  
HS codes of wood pulp.

Product category	Commodity code	Code details
Wood pulp	HS4701	Wood pulp, Mechanical wood pulp
	HS4702	Chemical wood pulp, Dissolving grade
	HS4703	Chemical wood pulp, soda or sulfite, other than dissolving grade
	HS4704	Wood pulp, chemical, other than sulfite, dissolving grade
	HS4705	Wood pulp obtained by a combination of mechanical and chemical pulping processes

imports remain negligible at less than 0.01%. Given China's status as a net importer with exports representing only 0.2% of imports, and since this study focuses on trade network structure, the data consolidation does not affect the findings.

To handle missing trade volume data, we used stratified mean imputation. The method works as follows: First, we grouped the raw data by HS code and transaction year. Then, for records with missing trade volumes within each HS-year group, we filled them using the arithmetic mean of non-missing values from the same group.

This study removed trade data below \$50 to improve data quality and computational efficiency. The results show that while the number of nodes and edges decreased by approximately 10%, network density increased by 12% and efficiency metrics improved by 3%–5%, with only a 4%–7% reduction in total trade volume. This indicates that low-value data primarily represent redundant connections, and the core network structure remains stable after removal, validating the rationality of this approach.

Ultimately, the trade data between countries is standardized in the format of importing country, exporting country, trade volume, and trade value. The HS codes are shown in Table 3.

## 2.2. Research framework

The assessment of network resilience can be approached from both a global and local perspective: globally, it focuses on the structural stability and efficiency of the network, i.e., structural resilience; locally, it concentrates on the ability of nodes to resist and recover from shocks, emphasizing the importance of individual nodes. Additionally, resilience assessment can be divided into two dimensions: static and dynamic. Static resilience assessment reveals the structural characteristics of the network when undisturbed, while dynamic resilience assessment examines the network's ability to adapt and recover under disruptive disturbances, which is crucial for the network's continued operation. This study starts with static network resilience and focuses on dynamic resilience, analyzing the global wood pulp trade network from the perspectives of structural resilience, node resilience, and destruction resistance. Since the network is a typical directed structure, its resilience assessment not only needs to consider trade relationships between countries but also the impact of trade volume. Based on existing research, we have constructed a comprehensive indicator system, as shown in Table 4, which includes weighted factors such as trade volume and trade intensity distance, aiming to provide a more accurate assessment of the resilience level of the global wood pulp trade network.

Based on this indicator system, we constructed a directed weighted trade network model for wood pulp products and systematically conducted an empirical study on network resilience. The research framework is shown in Fig. 1.

## 2.3. Graph theory model construction and evaluation indicators

### 2.3.1. Model construction

The global wood pulp trade countries (regions) are used as network nodes, with trade relationships between countries (regions) as edges, and trade volume and trade closeness as weights to construct the complex network model. The wood pulp trade network is defined as follows:

$$G_m = (V, E, W^1, W^2, T) \quad (1)$$

In the formula, the set  $V$  represents the collection of all countries (or regions); the set  $E$  represents the collection of trade relationships between countries (or regions);  $W^1$  represents the set of trade volume weights for edges between nodes;  $W^2$  represents the set of trade intensity relationship weights between nodes, and  $T$  represents the trade year.

In this paper, trade volume (in kilograms) is used as the edge weight for modeling to avoid inflation and price fluctuations, thereby accurately revealing the trade relationships and dependencies within the supply chain, which is crucial for analyzing network characteristics. At the same time, drawing on existing research (Huang et al., 2024), trade intensity relationships are introduced as edge weights to explore their impact on the shortest path length. The specific calculation formula for this edge weight is as follows:

$$w_{ij}^2 = 1 + \ln \text{Max}(w_{ij}^1) - \ln(w_{ij}^1) \quad (2)$$

In the formula,  $w_{ij}^1$  represents the trade intensity relationship between node  $i$  and node  $j$ ;  $\ln \text{Max}(w_{ij}^1)$  represents the maximum trade volume of edges in the network;  $\ln(w_{ij}^1)$  represents the trade volume of wood products exported from node  $i$  to node  $j$ . In reality, trade intensity relationships are undoubtedly influenced by more complex factors, such as political relations, geographical location, cultural differences, and many other difficult-to-quantify elements. However, within the specific analytical framework of this paper, we focus solely on trade volume as the core factor.

### 2.3.2. The structural resilience evaluation indicators

Based on existing research and the actual situation of global wood pulp trade, we have developed a comprehensive evaluation indicator system for network structural resilience, as shown in Table 5. The establishment of this system more accurately assesses the resilience level of the wood pulp supply network by carefully considering the impacts of edge weights such as supply volume and supply-demand tightness.

### 2.3.3. Node resilience evaluation indicators

Node resilience focuses on the characteristics of individual nodes in a network, affecting the network's resistance to damage and recovery ability in the event of local failures. The evaluation indicators are shown in Table 6.

### 2.3.4. Destruction resilience evaluation indicators

Destruction resilience characterizes the global features of network performance degradation caused by the continuous removal of nodes, providing an intuitive reflection of the network's stability and robustness under attack or failure scenarios. In this study, we simulate continuous node interruptions and analyze the network's destruction resilience by observing a series of cascading reactions triggered by overload cascading failures.

Assuming that the network experiences node disruption disturbances starting from time  $t_0$ , which triggers the underload cascading failure phenomenon, and this disturbance continues until all nodes fail at time  $t_1$ . During this process, we define  $P^h(t)$  as the network performance response function at time  $t$ . In particular, the area enclosed by the network performance curve and the time axis between  $t_0$  and  $t_1$  is quantified as the cumulative retained performance during the continuous node disruptions, which can be used to measure the

**Table 4**

Comprehensive indicator system for assessing the static and dynamic resilience of the global wood pulp trade network.

Type	Impact factor	Assessing the metrics	Impact on network resilience
Structural resilience	Transmissibility	Global efficiency	Global efficiency is an important metric for measuring the efficiency of information or resource transmission within a network, reflecting the ease of communication between nodes. Efficient networks can transmit information and resources more quickly, thereby enhancing overall network resilience. However, if a network relies too heavily on a few efficient paths, the failure of these paths can cause a significant drop in network performance, thereby affecting its robustness.
	Clustering	Average clustering coefficient	The average clustering coefficient is used to quantify the degree of connection tightness between neighboring nodes in a network, reflecting the network's local clustering. A high clustering coefficient indicates the presence of tight local clusters in the network, which helps improve local connectivity and transmission efficiency. However, overly tight local clusters may reduce the network's dependence on external clusters, thereby weakening global resilience.
	Hierarchicality	Degree distribution	Degree distribution describes the distribution of node degrees in a network and is an important indicator for analyzing network heterogeneity. A moderate hierarchical and flat structure helps balance robustness and vulnerability. However, if the degree distribution is overly concentrated (e.g., a few nodes have extremely high weighted degrees), the failure of these nodes may lead to a significant impairment of the network's overall functionality, affecting its stability.
	Homogeneity	Assortativity coefficient	The assortativity coefficient measures the tendency of nodes with similar attributes to be connected in a network. Assortative networks (where high trade volume nodes are connected to each other) can enhance the stability of hub nodes and provide quick recovery capabilities. On the other hand, disassortative networks (where high trade volume nodes are connected to low trade volume nodes) promote information and resource sharing but may lead to excessive dependence on hub nodes, potentially affecting the network's resilience and stability.
Node resilience	Vandalism resistance	In/Out degree & In/Out strength	The weighted degree reflects the importance of a node in the network. High-weighted degree nodes typically have stronger resistance to disruption and can maintain network functionality when some connections fail. However, high-weighted degree nodes may also become "single points of failure", and their failure can have a significant impact on the network, especially in networks with a highly concentrated degree distribution.
	Transit capacity	Betweenness centrality	Betweenness centrality measures the importance of a node as a bridge between other nodes. Nodes with high betweenness centrality can control key trade flows and enhance the network's transmission capacity. However, if these nodes fail, they may disrupt critical paths, significantly affecting the overall resilience of the network.
	Resilience	PageRank centrality	PageRank centrality is a node influence-based metric that quantifies nodal importance within networks, indicating a node's capacity to rapidly access and disseminate information flow. Nodes with elevated PageRank centrality demonstrate enhanced capability to mitigate risk propagation through efficient information interception and containment. However, excessive network reliance on these hub nodes creates systemic vulnerability — their potential failure could precipitate catastrophic declines in information transmission efficiency, ultimately compromising global network functionality.
Destruction resistance	Destruction resistance	Multi-point interruption retention value accumulation	The cumulative score of multi-point disruption retention value refers to the network's ability to maintain performance when facing disruption disturbances.

network's anti-damage resilience. The specific calculation formula is as follows:

$$R_{\text{resistance}}^h = \int_{t_0}^{t_1} P^h(t) dt \quad (3)$$

In the formula,  $R_{\text{resistance}}^h$  represents the retained value of the network performance in the process of continuous node disruptions based on  $P^h$ , which is related to the anti-damage resilience based on  $P^m$ . The specific network performance indicators are consistent with the vulnerability indicators of single-node failures, namely the global efficiency and the node strength of the largest connected subgraph, both of which are weighted indicators.

To specifically calculate the anti-damage resilience index, we assume that the node disruptions in the network occur at discrete time points. For simplification, it is assumed that the time interval between consecutive node disruptions is a constant step size  $\Delta t$ .

The different disruption sequences of nodes correspond to different permutations of the node set  $V$ . For a given permutation  $\sigma = \delta_1, \delta_2, \dots, \delta_n$ , we use  $P_{\delta_1}^h$  to represent the network performance after the failure of nodes up to the  $\delta_1$  node in the sequence, where  $i = 1, \dots, n$ , and  $n$  is the total number of original nodes.

Thus, we obtain the sequence that describes the network performance retention value, represented as:

$$(P_{\delta_1}^h, P_{\delta_2}^h, \dots, P_{\delta_n}^h) \quad (4)$$

In the above node failure sequence, if a node fails due to cascading effects from other nodes before it is scheduled to fail in the predetermined sequence, it should be removed from the sequence and the sequence should be reordered. After this operation, the resulting new sequence will have a number of nodes  $k$  that is smaller than the original total number of nodes  $n$  in the network.

$$(P_{\delta_1}^h, P_{\delta_2}^h, \dots, P_{\delta_k}^h) \quad (5)$$

We denote  $t_{\delta_0}$  as the starting time of the entire disruption process,  $t_{\delta_i}$  as the time when node  $\delta_i$  fails, and the continuous disruption interval as  $\Delta t$ . Due to the uncertainty of the network performance evolution curve, to simplify the calculation further the network performance curve between  $t_{\delta_{i-1}}$  and  $t_{\delta_i}$  is approximated linearly. That is the cumulative network performance during this period can be further represented as the area of trapezoidal approximation of network performance curve between time  $t_{\delta_{i-1}}$  and  $t_{\delta_i}$  along the time axis. The formula is as follows:

$$\int_{t_{\delta_{i-1}}}^{t_{\delta_i}} P^h(t) dt = \frac{(P_{\delta_{i-1}}^h + P_{\delta_i}^h) \times \Delta t}{2} \quad (6)$$

The formula for calculating the anti-damage resilience after the gradual failure of nodes is as follows:

$$R_{\text{resistance}}^h = \int_{t_{\delta_0}}^{t_{\delta_k}} P^h(t) dt = \frac{(P_{\delta_0}^h + P_{\delta_1}^h) \times \Delta t}{2} + \frac{(P_{\delta_1}^h + P_{\delta_2}^h) \times \Delta t}{2} + \dots$$

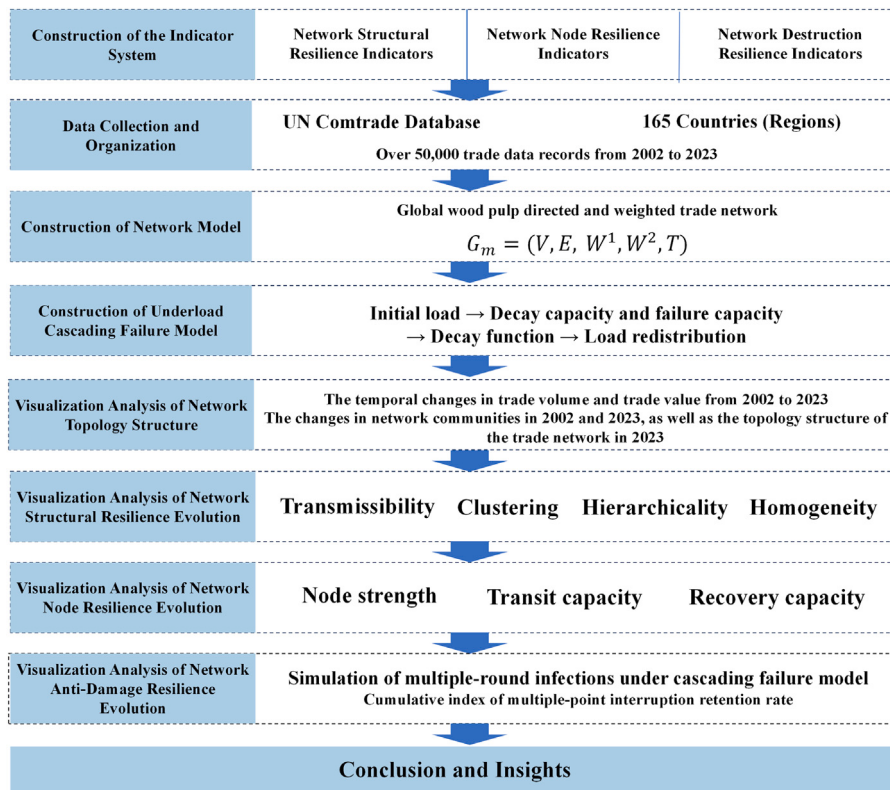


Fig. 1. Research framework flowchart.

$$+ \frac{(P_{\delta_{k-1}}^h + P_{\delta_k}^h) \times \Delta t}{2} \quad (7)$$

#### 2.4. The construction of the underload cascading failure model

The assessment of dynamic resilience in this study is built upon the underload cascading failure model previously proposed by our research team (Huang et al., 2025). This study fully retains its core framework and, by embedding a cumulative integral-based resilience assessment method into the model's output layer tailored to the heterogeneous characteristics of the wood pulp trade network, achieves a complete analytical chain from failure process simulation to dynamic resilience evaluation.

##### 2.4.1. Load and capacity settings

Before setting the export load decay function, the nodes are categorized into three types based on their import and export load characteristics: import-type (Type 1), import-export type (Type 2), and export-type (Type 3).

**Import-type nodes (Type 1):** The import load is greater than or equal to the export load. These nodes have three states for export load: normal, decay, and failure. The decay amount is determined by the ratio of import to export load and the node's decay state.

**Import-export type nodes (Type 2):** The import load is slightly smaller than the export load. These nodes also have three states for export load: normal, decay, and failure. The decay state decays proportionally based on the import load.

**Export-type nodes (Type 3):** The import load is much smaller than the export load. These nodes have only two states for export load: normal and decay, with no failure state.

Based on the above node classification and the node decay state function in formula (13), the export load decay function is further constructed.

The initial load of a node includes its import initial load, export initial load, and the initial load of its export neighboring edges. The specific formulas are as follows:

$$L_i^{in} = W_i^{1,in} \quad (8)$$

$$L_i^{out} = W_i^{1,out} \quad (9)$$

$$L_{ij} = w_{ij}^1 \quad (10)$$

In the formula,  $L_i^{in}$  and  $L_i^{out}$  and  $L_{ij}$  represent the initial import load, initial export load, and initial export load of node  $i$  to node  $j$ , respectively. They are equal to node  $i$ 's in-strength ( $W_i^{1,in}$ ), out-strength ( $W_i^{1,out}$ ), and the trade volume weight ( $w_{ij}^1$ ) of the export edge from node  $i$  to node  $j$ .

In the context of network resilience analysis, the decay capacity refers to the threshold below which a node begins to proactively reduce its export load in response to a decrease in its import load. This indicates the node's ability to buffer and adjust to disruptions in supply sources. The failure capacity, on the other hand, is the failure threshold capacity; when a node's import load falls below this value, the node fails and its export load to downstream nodes becomes zero. This reflects the node's tolerance or limit to disruptions in supply sources. The specific formulas for these capacities are as follows:

$$C_{i(dec)} = \alpha_1 L_i^{in} \quad 0 \leq \alpha_1 \leq 1 \quad (11)$$

$$C_{i(min)} = \alpha_2 L_i^{in} \quad 0 \leq \alpha_2 \leq \alpha_1 \leq 1 \quad (12)$$

In the formula,  $C_{i(dec)}$  and  $C_{i(min)}$  represent the decay capacity and failure capacity of the node, respectively;  $\alpha_1$  is the decay coefficient, a key parameter for adjusting decay capacity during simulation;  $\alpha_2$  is the failure coefficient, a key parameter for adjusting failure capacity during simulation.

**Table 5**  
Indicators related to structural resilience.

Indicator name	Formula	Description
Global efficiency	$E = \frac{1}{N(N-1)} \sum_{i \neq j} \frac{1}{d_{ij}}$	The unweighted global efficiency $E$ refers to the average of the reciprocals of the shortest path lengths $d_{ij}$ between all nodes in an unweighted network, measuring the information transmission speed and capacity of the unweighted network. The weighted global efficiency $E_{w^2}$ is the global efficiency calculated by considering the trade intensity relationship weights in addition to the unweighted global efficiency.
	$E_{w^2} = \frac{1}{N(N-1)} \sum_{i \neq j} \frac{1}{d_{w^2 ij}^{-2}}$	
Average clustering coefficient	$C_i = \frac{1}{k_i(k_i-1)} \sum_{s \neq i} \sum_{t \neq s \neq i} T_{st}$	The unweighted average clustering coefficient $C$ is the arithmetic mean of the unweighted clustering coefficients $C_i$ of all nodes, reflecting the degree of close clustering between nodes in the unweighted network. $T_{st}$ represents the supply quantity between node $s$ and node $t$ ; $k_i$ represents the degree of node $s$ . The weighted average clustering coefficient $C_{w^1 i}$ is based on the unweighted average clustering coefficient, but considers the edge weights.
	$C = \frac{1}{N} \sum_{i=1}^N C_i$	
	$C_{w^1 i} = \frac{1}{k_i(k_i-1) \text{Max}(w_{ij}^1)} \sum_{s \neq i} \sum_{t \neq s \neq i} T_{w^1 st}$	
	$C_{w^1} = \frac{1}{N} \sum_{i=1}^N C_{w^1 i}$	
Assortativity coefficient	$r = \frac{K^{-1} \sum_i (j_i k_i) - \left[ K^{-1} \sum_i \frac{1}{2} (j_i + k_i) \right]^2}{K^{-1} \sum_i \frac{1}{2} (j_i^2 + k_i^2) - \left[ K^{-1} \sum_i \frac{1}{2} (j_i + k_i) \right]^2}$	The assortativity coefficient is a Pearson correlation coefficient based on “degree”, used to measure the relationship between connected node pairs. The unweighted assortativity coefficient $r$ refers to the tendency of countries (regions) in the network to connect with other countries (regions) that have similar total supply quantities, without considering supply weight. Here, $j_i$ and $k_i$ represent the degrees of the connected nodes and of the edge. The weighted assortativity coefficient $r_{w^1}$ , on the other hand, takes into account supply-weighted situations.
	$r_{w^1} = \frac{H^{-1} \sum_i w_i^1 (j_i k_i) - \left[ H^{-1} \sum_i \frac{1}{2} w_i^1 (j_i + k_i) \right]^2}{H^{-1} \sum_i \frac{1}{2} w_i^1 (j_i^2 + k_i^2) - \left[ H^{-1} \sum_i \frac{1}{2} w_i^1 (j_i + k_i) \right]^2}$	
	$H = \sum_i w_i^1$	
Degree distribution	$K_i = C(K_i^*)^\alpha$	The measurement of hierarchy is reflected through the network degree distribution index. The unweighted degree distribution refers to the node degree probability distribution without considering supply weight. $K_i^*$ represents the rank of node $i$ 's degree among all node degrees; $C$ is the proportional constant; and $\alpha$ is the slope of the degree distribution curve, which is used to measure the network's hierarchical structure. The weighted degree distribution refers to the node degree probability distribution, considering supply weight.
	$\ln K_i = \ln C + \alpha \ln(K_i^*)^\alpha$	
	$K_{w^1 i} = C_{w^1} (K_{w^1 i}^*)^\alpha$	
	$\ln K_{w^1 i} = \ln C_{w^1} + \alpha \ln(K_{w^1 i}^*)^\alpha$	

Different nodes have different decay and failure coefficients. Further, the node decay state function is set as follows:

$$f_i(t) = \begin{cases} 0 & L_i^{in}(t) \geq C_{i(dec)} \\ \frac{L_i^{in}(t)}{L_i^{in}} & C_{i(min)} \leq L_i^{in}(t) \leq C_{i(dec)} \\ 1 & L_i^{in}(t) \leq C_{i(min)} \end{cases} \quad (13)$$

In the formula,  $f_i(t)$  represents the attenuation state parameter, where 1 indicates a failure state and 0 indicates a normal state;  $\alpha_2 \leq f_i(t) \leq \alpha_1$  denotes the attenuation state.

#### 2.4.2. Decay function

(1) Export Load Decay Function for Import-Type (Type 1) Nodes The export decay of import-type nodes is influenced by both the import-export load ratio and the node's decay state. The function is as follows:

$$\Delta L_i^{out}(t) = \begin{cases} 0 & f_i(t) = 0 \\ L_i^{out} * (1 - \alpha_3 * f_i(t)) & 0 < f_i(t) < 1 \\ L_i^{out} & f_i(t) = 1 \end{cases} \quad (14)$$

In the formula,  $\Delta L_i^{out}(t)$  represents the export attenuation amount of node  $i$  at time  $t$  (the same applies below): When  $f_i(t) = 0$ , the node is in a normal state, and the export attenuation amount is 0; When  $f_i(t) = 1$ , the node is in a failure state, and the export load drops to 0; When  $0 < f_i(t) < 1$ , the export attenuation load is influenced by both  $f_i(t)$  and  $\alpha_3$ .  $\alpha_3$  represents the ratio of the node's export load to its import load. Generally, if the node's import load is greater than or equal to the export load, the  $\alpha_3$  calculation formula is as follows:

$$\alpha_3 = \frac{1}{1 + \ln(W_i^{1,in}) - \ln(W_i^{1,out})} \quad W_i^{1,out} \leq W_i^{1,in} \quad (15)$$

It can be seen that the value of  $\alpha_3$  depends on the logarithmic difference between the import and export volumes. When  $W_i^{1,in} = W_i^{1,out}$ , the logarithmic difference is zero, at which point  $\alpha_3 = 1$ , and the attenuation ratio of the export load is equal to the attenuation ratio of the import load,  $1 - f_i(t)$ . This reflects that when the import and export loads are balanced, the attenuation and failure effects on imports and exports are consistent. When  $W_i^{1,in} > W_i^{1,out}$ , the logarithmic difference is positive, at which point  $\alpha_3 < 1$ , and decreases as the difference between import and export volumes increases. At this time, the export load's attenuation ratio  $1 - \alpha_3 * f_i(t)$  is significantly higher than the import load's attenuation ratio  $1 - f_i(t)$ . This is because the node is more dependent on the import load, and when the node's supply source fails, the impact on the export load becomes more significant. By adjusting  $\alpha_3$ , the model can more accurately reflect the attenuation differences caused by the differing import and export load ratios.

In summary, the  $\alpha_3$  parameter plays a key role in the export attenuation model for import-type nodes. It adjusts the attenuation degree of the export load based on the import-export load ratio, enabling the model to more accurately describe the attenuation behavior of nodes under different states. This is crucial for understanding and analyzing the impact of node failures on overall network performance in complex networks.

(2) Export-Load Attenuation Function for Import-Export Nodes (Type 2) For import-export type nodes, the import load is slightly smaller than the export load, but it is greater than or equal to the product of the export load and the control coefficient  $\alpha_4$ . In this study,  $\alpha_4$  is set to 1/5. The export load attenuation function for such nodes is

**Table 6**  
Node resilience related indicators.

Indicator name	Formula	Description
Out degree & Out strength	$W_i^{\text{out}} = \sum_{j=1}^N w_{ij}$ $W_i^{1,\text{out}} = \sum_{j=1}^N w_{ij}^1$	The out-degree $W_i^{\text{out}}$ of a node refers to the sum of the number of edges from node $i$ pointing to other nodes. The out-strength $W_i^{1,\text{out}}$ of a node refers to the sum of the export trade volume weights ( $W_{ij}^1$ ) from node $i$ pointing to other nodes.
In degree & In strength	$W_i^{\text{in}} = \sum_{j=1}^N w_{ij}$ $W_i^{1,\text{in}} = \sum_{j=1}^N w_{ij}^1$	The in-degree $W_i^{\text{in}}$ of a node refers to the sum of the number of edges pointing to node $i$ from other nodes. The in-strength $W_i^{1,\text{in}}$ of a node refers to the sum of the import trade volume weights ( $W_{ij}^1$ ) pointing to node $i$ from other nodes.
Betweenness centrality	$BC_i = \sum_{s \neq i \neq t} \frac{n_{st}^i}{g_{st}}$ $BC_{w^2,i} = \sum_{s \neq i \neq t} \frac{n_{w^2,st}^i}{g_{w^2,st}}$	Betweenness centrality refers to the number of shortest paths passing through a node divided by the total number of shortest paths between other pairs of nodes, measuring the importance and influence of a country (region) in the network from the perspective of its “bridge” role. Unweighted betweenness $BC_i$ centrality refers to the betweenness centrality calculated without considering trade relationship weights. Weighted betweenness centrality $BC_{w^2,i}$ refers to the betweenness centrality calculated considering the trade tightness relationship weights.
PageRank centrality	$PR_i = \alpha \sum_{j \in \text{In}(i)} \frac{PR_{w^1,j}}{k_i^{\text{out}}} + (1 - \alpha) \frac{1}{N}$ $PR_{w^1,i} = \alpha \sum_{j \in \text{In}(i)} \frac{w_{ji} * PR_{w^1,j}}{k_i^{\text{out}}} + (1 - \alpha) \frac{1}{N}$	PageRank centrality is a node importance measure calculated by simulating a random walker who, with probability $\alpha$ , moves along the outgoing edges of the current node to neighboring nodes, and with probability $(1 - \alpha)$ , jumps to a random node in the network. This value depends on the average importance of the nodes pointing to it and the global visibility of the node in the network. Unweighted PageRank centrality disregards edge weights, treating all outgoing edges as equally probable paths. The node's importance is solely dependent on its topological connectivity, namely the number of incoming edges and its own PageRank value. Weighted PageRank centrality incorporates trade volume weights, factoring edge weights into the jump probability calculation. In this case, the random walker is more likely to choose edges with higher trade volumes to transition. Node importance is not only influenced by the number of incoming edges but also directly linked to the trade strength represented by the edge weights.
Eigenvector centrality	$EC_{w^1,i} = \frac{1}{\lambda} \sum_{j=1}^N w_{ij} EC_{w^1,j}$	Weighted eigenvector centrality $EC_{w^1,i}$ is a centrality measure that, considering trade volume weights, evaluates the importance of node $i$ in the network based on the importance of its neighboring nodes $EC_{w^1,j}$ using eigenvector analysis. $\lambda$ represents the largest eigenvalue of the network's adjacency matrix.

as follows:

$$\Delta L_i^{\text{out}}(t) = \begin{cases} 0 & f_i(t) = 0 \\ L_i^{\text{in}} - L_i^{\text{in}}(t) & 0 < f_i(t) < 1 \\ L_i^{\text{out}} & f_i(t) = 1 \end{cases} \quad (16)$$

In the formula,  $\Delta L_i^{\text{out}}(t)$  represents the export attenuation of node  $i$  at time  $t$ : When  $f_i(t) = 0$ , the node is in the normal state, and the export attenuation is 0; When  $f_i(t) = 1$ , the node is in the failure state, and the export load is reduced to 0; When  $0 < f_i(t) < 1$ , the export attenuation load  $L_i^{\text{in}}$  equals the initial import load  $L_i^{\text{in}}(t)$  minus the import load at time  $t$ , meaning the export load attenuation is equal to the import load attenuation.

(3) Export-type (Type 3) Node Export Load Attenuation Function  
Export-type nodes primarily export goods, with import load much smaller than export load. In this study, nodes where the import load is smaller than the export load multiplied by  $\alpha_4$  are classified as this type. The export load attenuation of such nodes has only two states: normal and attenuation, without a failure state. The export load attenuation function for these nodes is as follows:

$$\Delta L_i^{\text{out}}(t) = \begin{cases} 0 & f_i(t) = 1 \\ L_i^{\text{in}} - L_i^{\text{in}}(t) & 0 < f_i(t) \leq 1 \end{cases} \quad (17)$$

In the formula,  $\Delta L_i^{\text{out}}(t)$  represents the export load attenuation for node  $i$  at time  $t$ : When  $f_i(t) = 0$ , the node is in a normal state, and the export attenuation is 0; When  $0 < f_i(t) < 1$ , the export load attenuation is equal to the initial import load  $L_i^{\text{in}}$  minus the import load  $L_i^{\text{in}}(t)$  at time  $t$ . However, since the export load is much larger than the import load, the impact of the attenuation on the export is minimal.

#### 2.4.3. Export load reallocation

In a trade network, when a node fails or decays, the material or load that should have been provided by that node cannot be fully transmitted to the downstream nodes, causing a reduction in export load. This reduction amount,  $\Delta L_i^{\text{out}}(t)$ , needs to be allocated to downstream nodes according to specific rules. Two situations need to be considered: First, if a node completely fails, the export load between the node and all its adjacent nodes becomes zero, i.e.,  $\Delta L_i^{\text{out}}(t) = W_i^{\text{out}}$ , and the edge load between node  $i$  and its adjacent nodes also becomes zero, i.e., edge load reduction  $\Delta L_{ij} = W_{ij}^1$ . Second, if a node decays but does not fail, its export load is inversely distributed to the downstream nodes according to the strength of their business relationships. This study proposes that, in the case of underload failure, nodes with weaker relationship strength should be allocated more of the decay load, starting with the least important trade relationship nodes until the entire decay amount is distributed. Based on this, the importance of trade partnerships between nodes is defined as follows:

$$O_{ij} = W_{ij}^1 * EC_j \quad (18)$$

In the formula,  $O_{ij}$  represents the importance of trade partnerships,  $W_{ij}^1$  is the trade volume between node  $i$  and node  $j$ , and  $EC_j$  is the feature vector centrality of node  $i$ 's export neighbor node  $j$ . Then, the trade partnership importance  $O_{ij}$  of node  $i$ 's export neighbors is sorted in ascending order as  $\sigma = \varepsilon_1, \varepsilon_2, \dots, \varepsilon_{k_i}$ , where  $k_i$  is the out-degree of node  $i$ . Based on the importance of nodes, the decay amount is allocated in increasing order, resulting in a sequence describing the remaining allocable decay amount,  $R_{i\varepsilon_j}$ , as follows:

$$(R_{i\varepsilon_1}, R_{i\varepsilon_2}, \dots, R_{i\varepsilon_{k_i}}) \quad (19)$$

$$R_{ie_j} = \Delta L_i^{\text{out}} - \Delta L_{ie_1} - \Delta L_{ie_2} - \dots - \Delta L_{ie_{j-1}} \quad (20)$$

In the formula,  $R_{ie_j}$  represents the remaining allocable decay amount on the export edge from node  $i$  to neighboring node  $\epsilon_j$ , and  $\Delta L_{ie_j}$  represents the allocated decay amount on the export edge from node  $i$  to neighboring node  $\epsilon_j$ . The allocation of the decay amount for the  $t$ th period can follow the following rule, starting from the first node  $\epsilon_j$  ( $j = 1$ ) in the  $\sigma$  sequence:

(1) Calculate the load decay allocation for node  $\epsilon_j$ : If  $\frac{k_i - \epsilon_j}{k_i} > f_i(t)$ , compare  $W_{ie_j} * \frac{k_i - \epsilon_j}{k_i}$  with the remaining distributable decay amount  $R_{ie_j}(t)$ . If  $W_{ie_j} * \frac{k_i - \epsilon_j}{k_i}$  is greater, then set  $\Delta L_{ie_j}(t) = W_{ie_j} * \frac{k_i - \epsilon_j}{k_i}$ ; otherwise, set  $\Delta L_{ie_j}(t) = R_{ie_j}(t)$ . If  $\frac{k_i - \epsilon_j}{k_i} \leq f_i(t)$ , compare  $W_{ie_j} * f_i(t)$  with the remaining distributable amount. If  $W_{ie_j} * f_i(t)$  is greater, set  $\Delta L_{ie_j}(t) = R_{ie_j}(t)$ ; otherwise, set.

(2) Calculate the remaining distributable decay amount for the next export edge of the neighboring node:

$$R_{ie_{j+1}}(t) = \Delta L_i^{\text{out}}(t) - \Delta L_{ie_1}(t) - \Delta L_{ie_2}(t) - \dots - \Delta L_{ie_{j-1}}(t) - \Delta L_{ie_j}(t) \quad (21)$$

(3) Return to (1), and calculate the load decay distribution for the next outbound neighbor edge, until the load decay distribution for all outbound neighbor edges of node  $i$  is completed. Since the load redistribution process causes changes in the load of adjacent nodes, the next step is to assess the import load of the next-level node and proceed with the next round of load distribution. This process continues until the underload cascading failure process stops. The specific steps are as follows:

(a) To compute the export load  $L_{ij}(t+1)$  from node  $i$  to node  $j$  in the  $t+1$  period, you would typically follow these steps:

$$L_{ij}(t+1) = L_{ij}(t) - \Delta L_{ij}(t) \quad (22)$$

(b) Calculate the import load of all nodes in the new cycle network:

$$L_j^{\text{in}}(t+1) = \sum_{i \in \theta(j)} L_{ij}(t+1) \quad (23)$$

### 3. Results analysis

#### 3.1. Evolution analysis of static network resilience

##### 3.1.1. Network overall feature analysis (figures/tables moved to appendix)

The global wood pulp trade network showed decreasing nodes but increasing connections during 2002–2023 (Fig. A.1), reflecting ongoing structural adjustments where trade hubs gained greater importance while trade cooperation and interconnectivity strengthened.

Global wood pulp trade volume showed steady growth from 2020 to 2023 (Fig. 2), reflecting its essential industrial demand characteristics, while trade value was significantly affected by price fluctuations. The 2008 financial crisis caused a delayed impact with trade value sharply declining in 2009, whereas the 2020 pandemic induced immediate shocks to trade value, consistent with Woods (2014) crisis transmission theory. Subsequent analyses used trade volume data to eliminate interference from inflation and price factors.

From 2002 to 2023, the global wood pulp trade network underwent significant restructuring (Fig. A.3), as evidenced by the following: China became the largest importer, reflecting the rapid expansion of the paper industry; Brazil surpassed Canada as the leading exporter, highlighting the advantages of tropical fast-growing forests; Indonesia emerged as the third-largest exporter, demonstrating the success of plantation-based economies; meanwhile, trade concentration intensified, posing challenges for smaller or emerging producer and importer countries.

The community structure of the global wood pulp trade network underwent significant reorganization from 2002 to 2023 (Fig. A.4). Brazil replaced the U.S. and Canada as the largest supply hub. China

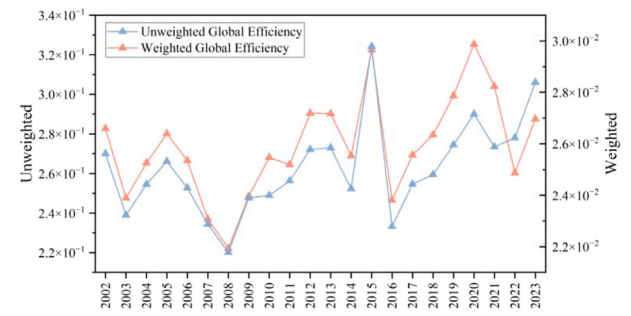


Fig. 2. Evolution of global efficiency of network from 2002 to 2023.

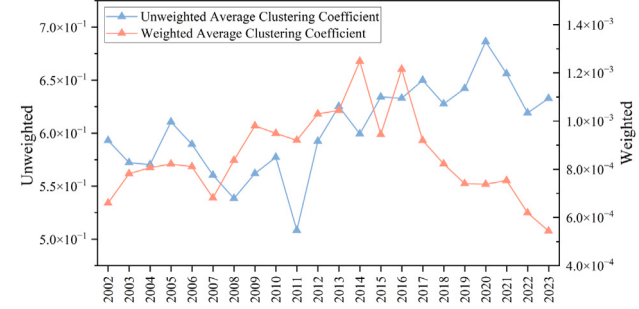


Fig. 3. Evolution of average clustering coefficient of network from 2002 to 2023.

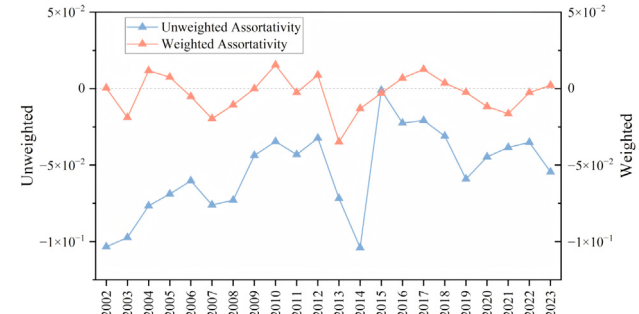
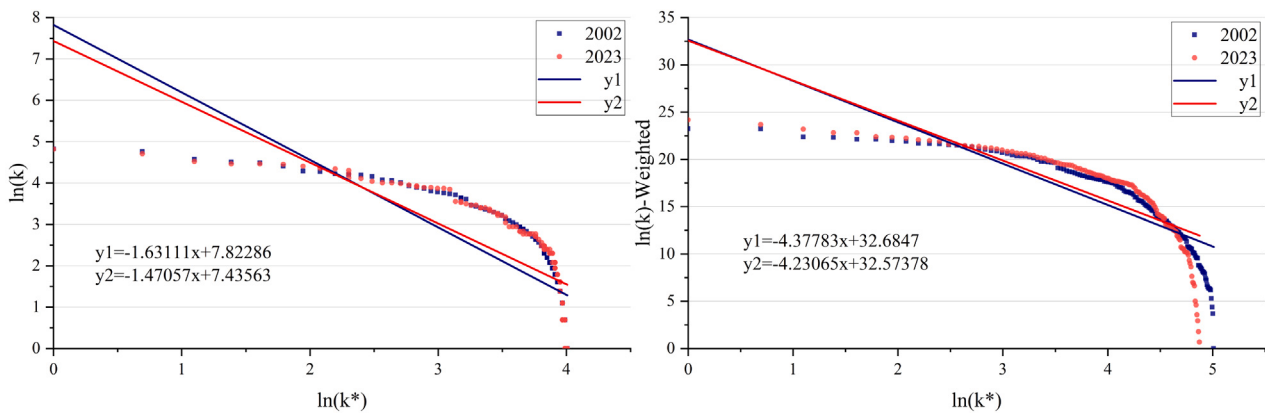


Fig. 4. Evolution of assortativity of network from 2002 to 2023.

formed an independent trade cluster. Multi-polarization increased the number of communities from three to five. These changes indicate that the traditional supply–demand binary model is evolving into a more complex multilateral trade relationship. However, over-reliance on regional core countries may increase systemic risks.

##### 3.1.2. Evolution analysis of static structural resilience

This section analyzes the structural resilience and evolution of the global wood pulp trade network from four dimensions: transitivity, clustering, hierarchy, and assortativity. Fig. 2 shows that both unweighted and weighted global efficiency increased from 2002 to 2023, indicating a significant improvement in network transmission efficiency. In Fig. 3, the unweighted clustering coefficient rises while the weighted average clustering coefficient first increases and then decreases, reflecting closer trade relationships among countries but a gradual dispersion of clusters among high-trade-volume nations. Fig. 4 illustrates negative unweighted assortativity, showing a “small-country dependence on hubs” characteristic, whereas weighted assortativity remains close to zero, suggesting a relatively balanced network structure. Fig. 5 reveals that the degree distribution follows a power-law distribution. Compared to 2002, the network hierarchy weakened by



**Fig. 5.** Evolution of degree distribution of network in 2002 and 2023.

2023, with diversification increasing, enhancing resistance to targeted attacks but reducing robustness against random disturbances.

Figs. 2 and 3 show that after the 2008 financial crisis, global efficiency and clustering coefficient continued their existing trends and accelerated in 2009, reflecting the time-lagged effect of market self-optimization. In contrast, the 2020 COVID-19 pandemic caused immediate surges in these metrics, demonstrating the “supply assurance priority” emergency response mechanism. This difference validates Woods’ theory, indicating that economic crises gradually optimize networks through market adjustments, while public health emergencies directly strengthen network resilience through institutional interventions.

### 3.1.3. Evolution analysis of static nodal resilience

Figs. A.5 to A.8 show changes in node degree and centrality in the wood pulp trade network from 2002 to 2023. Overall, the importance of China and Brazil has significantly increased. In terms of exports, Brazil replaced Canada as the largest exporter. Meanwhile, China’s role as an import hub has strengthened. Its in-degree and in-strength have risen sharply, surpassing the United States to become the largest importer, widening the gap with other traditional importers. Additionally, China’s unweighted and weighted betweenness centrality have grown significantly, highlighting its key role in the global wood pulp trade network. Finally, Pakistan’s connectivity and importance in the global trade network have notably improved, with increased PageRank centrality, making it an emerging influential node.

To provide a comprehensive and in-depth analysis of the changes in node resilience, we integrated four key indicators — out-strength, in-strength, weighted betweenness centrality, and weighted closeness centrality — into a single figure (Fig. 6). This allowed for a detailed depiction of the distribution of core nodes in 2002 and 2023. The goal is to explore the evolution patterns and characteristics of node resilience through a comparative analysis.

According to Fig. 6, the global wood pulp trade network underwent significant changes between 2002 and 2023. China emerged as a central node with comprehensive growth — its import strength increased 5.14-fold to 32.1 billion, export strength rose 1.63-fold to 60 million, weighted betweenness centrality grew 3.54-fold to 0.11, and PageRank centrality improved 1.28-fold to 0.094. These metrics confirm China’s evolution into a global trade hub with both resource absorption and transit capabilities. Brazil demonstrated distinctive transitional characteristics. Its export strength surged 4.19-fold while weighted betweenness centrality increased 3.26-fold, indicating enhanced regional supply chain output capacity. However, a 0.57-fold decline in import strength revealed weakening global resource attraction. The United States maintained its dual role as both import and export hub, though its relative network importance diminished amid the rapid rise of emerging economies like China.

The global wood pulp trade network has now established a tripartite structure centered on China, Brazil, and the United States. China’s exceptional performance in transit functionality and nodal significance is actively reshaping the power dynamics of the global wood pulp trade system.

### 3.2. Cascading failure pathways in core exporters under underloading

After analyzing the characteristics of the pulp trade network, we further explored its network resilience and its changes, with a focus on the underloading cascading failures triggered by node disruptions. Using Python tools and based on the underloading cascading failure model, we conducted a simulation to capture the failure diffusion paths following node disruptions. Given that Brazil is the largest exporter of pulp, we used Brazil as the initial failure node for the cascading failure transmission simulation. The failure transmission process obtained from the simulation aligns with the actual trade situation, as shown in Fig. 8, which validates the accuracy of the cascading failure model (see Fig. 7).

As shown in Fig. 8, 12 countries, including China, the United States, and Australia, experienced immediate import shortages due to their dependence on Brazil’s export supply after the initial failure. This caused their import load to fall below the failure threshold, turning them into the first-round failure nodes. Japan, Thailand, and 20 other countries, due to their strong trade dependency on the first-round failure nodes, saw further declines in their import load, triggering the second round of failure. Poland, France, and other countries, due to the chain reaction caused by the supply chain disruption, led to a significant reduction in trade volume in 32 countries, while only 62 countries were minimally affected.

To analyze the propagation characteristics of underload cascading failures, we simulated the disruption of Canada, the second-largest exporter (Fig. 8). The results show that the failure process occurs in three stages: first, Canada fails; then the United States is affected; followed by the spread to 15 countries, including Japan, Thailand, and Mexico. This indicates that the failure starts from a core supplier and gradually spreads to secondary nodes and broader regions. North American nodes are impacted first, followed by synchronized failures in multiple countries across Asia and the Americas, demonstrating cross-regional synchronization and hierarchical progression. Additionally, 35 countries, including Germany, Australia, France, and China, are also affected, covering major economies across four continents, highlighting the extensive chain reaction triggered by the disruption of a core supply node.

Brazil and Canada’s failure rapidly triggered large-scale cascading failures, indicating the high dependency of the global pulp trade network on core exporting countries. This “single point of failure” risk exposes the vulnerability of the network structure, particularly the issue of export concentration.

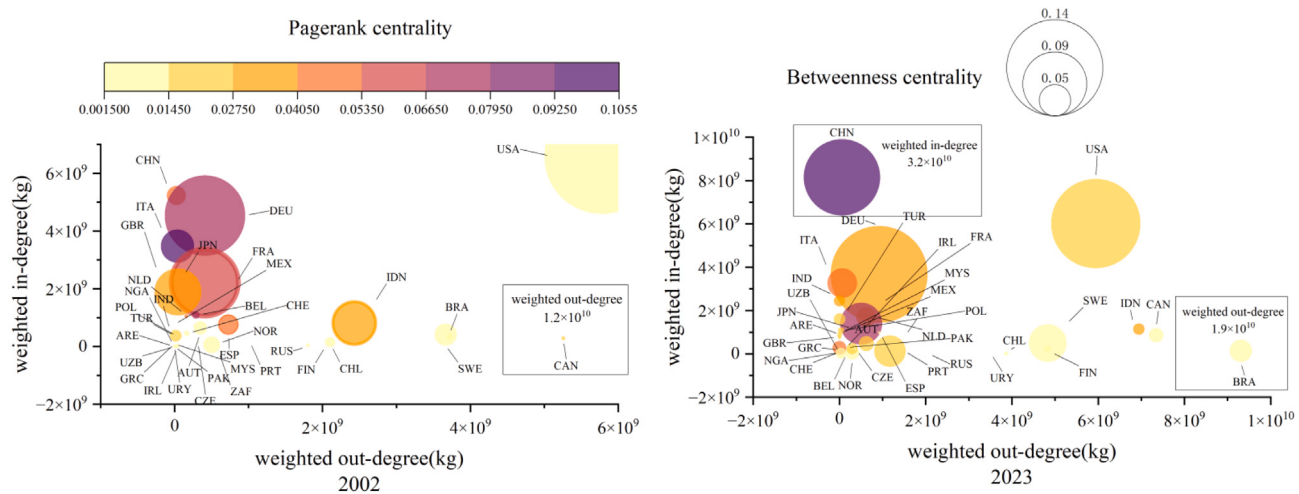


Fig. 6. Evolution trend of core node resilience.

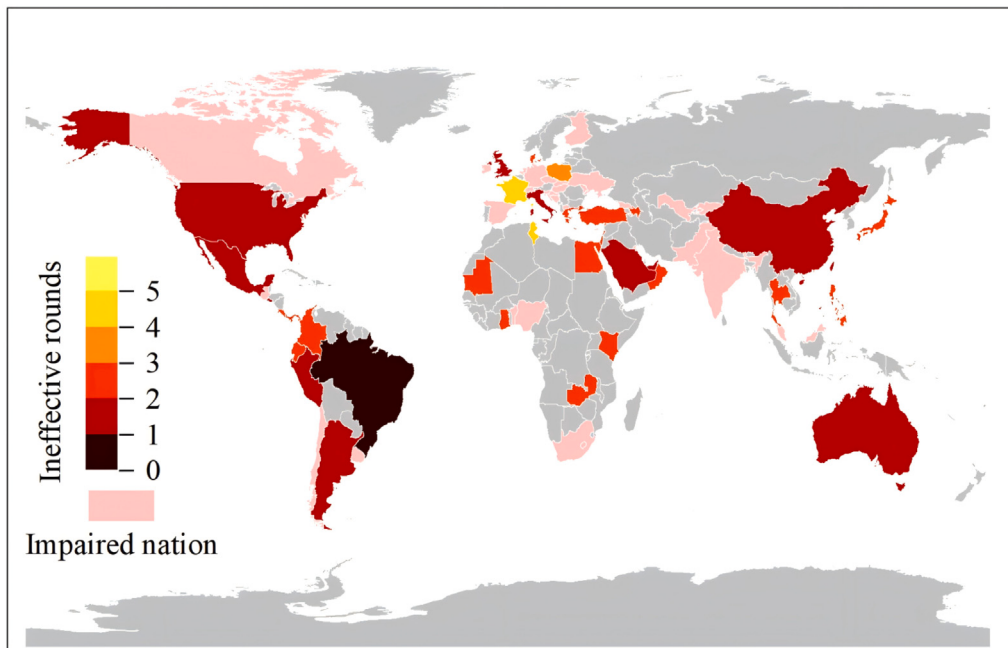


Fig. 7. 2023 BRA underload cascade failure conduction map.

### 3.3. Dynamic resilience evolution under multiple node disruptions

Four simulation strategies were employed to assess the global wood pulp trade network's resilience to sequential node disruptions in 2023: random disturbance, strength rank-based node removal, betweenness centrality rank-based removal, and PageRank centrality rank-based removal. Fig. 9 demonstrates differential network performance degradation patterns across these intervention strategies.

Fig. 9 demonstrates the effects of node removal strategies on wood pulp trade network performance. Analysis reveals significantly higher network performance retention rates under random disturbance compared to targeted removal strategies (strength-based, betweenness centrality-based, and PageRank centrality-based interventions), indicating reduced systemic vulnerability to random disruptions.

From the figure, it is clear that whether nodes are interrupted based on out-strength or betweenness centrality, the network's global efficiency and the retention rate of the maximum connected component's node strength are much lower than under the other strategies. Notably,

when the top 10 nodes are interrupted, the network's performance drops rapidly. This not only confirms the critical role of major exporting countries in the network, where their failure quickly and significantly weakens network performance, but also highlights the essential role of core nodes acting as bridges in maintaining the stability of the network. The strategy of interrupting nodes based on PageRank centrality results in a relatively higher retention rate, but it is still far lower than the network performance retention rate under the random interruption strategy. This suggests that PageRank centrality, to some extent, reflects the significant influence of nodes.

For quantitative assessment of performance degradation during sequential node removal, Table 7 provides cumulative network performance retention percentages relative to baseline values (note: distinct from structural resilience metrics).

As seen from the table above, deliberate disruption has far more destructive impact on the network compared to random disruption. Countries should strengthen network security and emergency response capabilities to prevent deliberate attacks; at the same time, diversify supply channels to reduce dependence on a single source and

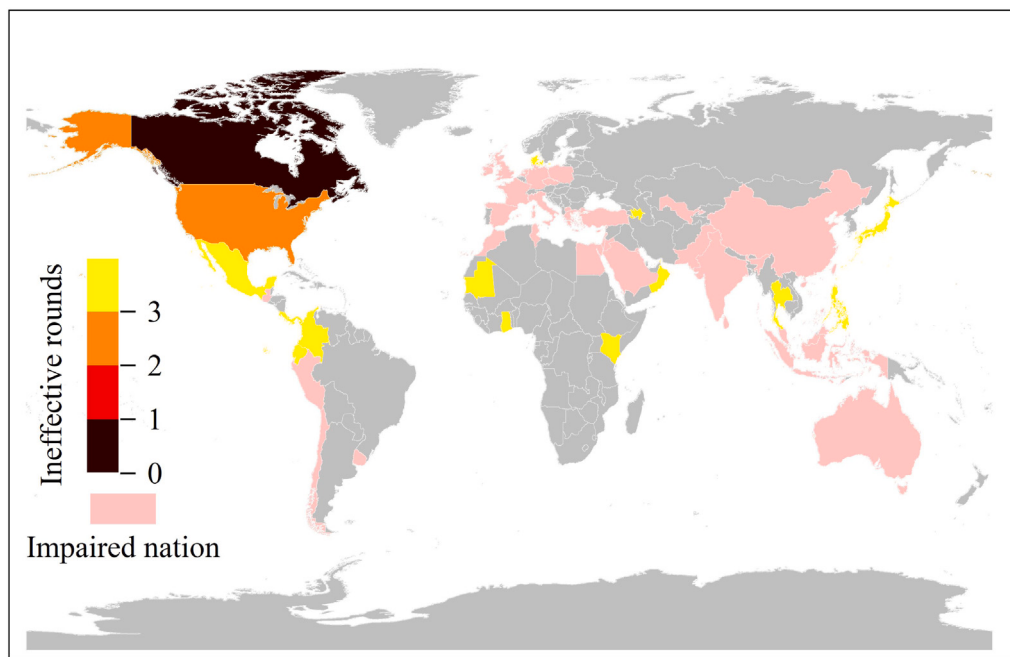


**Fig. 8.** 2023 CAN underload cascade failure conduction map.

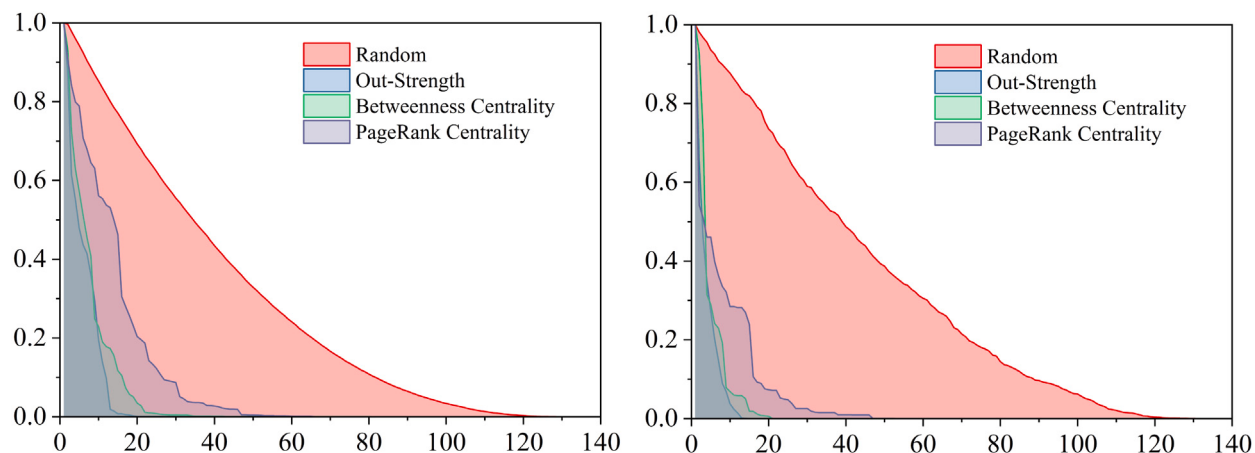


**Fig. 9.** Simulation results of multi-point outage network performance retention rate in 2023.

**Table 7**  
The cumulative retention performance proportion in 2023.

	Random disruption	Disruption by node outstrength	Disruption by betweenness centrality	Disruption by PageRank centrality
Global efficiency	29.4%	3.9%	5.0%	9.8%
Node Strength in the largest connected subgraph	32.8%	2.2%	3.0%	5.1%

mitigate disruption risks caused by political or economic factors; furthermore, enhance network monitoring and early warning mechanisms to improve supply flexibility and resilience in response to emergencies.

Leveraging Python-based computational frameworks, we conducted multi-node underload cascading failure simulations on the global wood pulp trade network (2002–2023) following Eq. (7). The systematic implementation of three disruption strategies-random failures, degree-based targeted attacks, and betweenness centrality-prioritized

removals-revealed distinct evolutionary patterns in network survivability.

**Fig. 10** characterizes the dynamic structural resilience evolution of the global wood pulp trade network (2002–2023) through two key patterns:

(1) Strategy-dependent resilience variance: Network resilience exhibits marked divergence across removal strategies. Both random node removal and betweenness centrality-based strategies drive progressive performance decline, underscoring growing topological dependence on

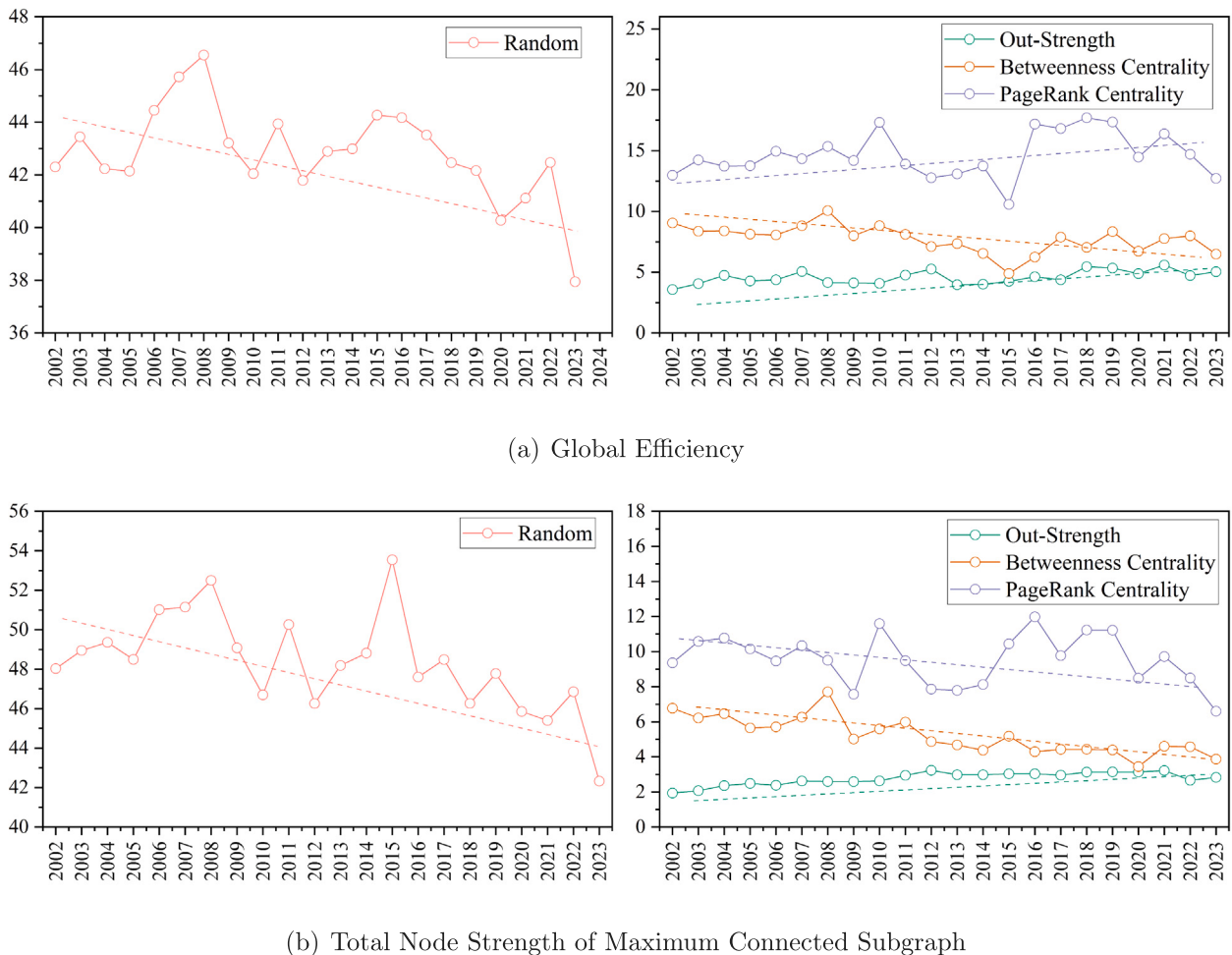


**Fig. 10.** Simulation results of network dynamic resilience evolution from 2002 to 2023.

high-betweenness bridge nodes. Conversely, PageRank centrality-based removal yields superior resilience, indicating reduced systemic vulnerability through balanced influence distribution. The enhanced resilience under out-strength prioritization confirms supply chain structural shifts from centralized to distributed architectures, improving single-point failure resistance.

(2) Temporal shock response asymmetry: External disruptions demonstrate chronologically distinct impacts. The 2009 resilience decline captures delayed effects of the 2008 financial crisis, consistent with Woods (2014)'s delayed transmission paradigm. Contrastingly, the 2020 pandemic induced acute resilience contraction, revealing fundamentally distinct crisis propagation mechanisms between economic and public health shocks.

#### 3.4. Comparative dynamic resilience under diverse scenarios

In the dynamic resilience simulation of the wood pulp trade network, the decay threshold and failure threshold are key control parameters. The decay threshold reflects the node's anti-degradation ability, while the failure threshold reflects the node's anti-damage resilience. Since both the decay threshold and failure threshold characterize the node's anti-damage capability to varying degrees, experiments have repeatedly shown that changes in  $\alpha_1$  do not significantly affect anti-damage resilience. Therefore, this paper focuses on the graded simulation of  $\alpha_2$  for in-depth discussion (see Table 8).

This study maintains initial parameter configurations while executing multi-scenario simulations through Python-based computational implementation, guided by the mathematical framework in Eq. (7). The simulations adopt parameter values specified in the referenced table to systematically analyze the global wood pulp trade system's topological responses. Fig. 11 delineates the resulting network characteristics across parameter combinations, providing comprehensive visualization of 2023 structural configurations.

From Fig. 11, it is evident that under different failure coefficient settings, the differences in network performance retention rates are quite pronounced, indicating that a node's failure capability directly impacts the network's anti-damage resilience. In the metric of global network efficiency, changes in the failure coefficient have a particularly significant effect on the network's anti-damage resilience, with resilience clearly increasing as the failure coefficient rises. In contrast, the metric of the total strength of the largest connected subgraph shows a less pronounced effect, but it still demonstrates a negative correlation between the network's anti-damage resilience and the failure coefficient.

Fig. 12 shows that lowering the failure threshold significantly enhances the network's resilience. Using global efficiency as a metric, resilience against failure increased by 5.57 times, indicating a substantial enhancement in redundancy and alternative routing capabilities for information transmission. Meanwhile, resilience based on the node strength of the largest connected subgraph increased by 3.59 times, demonstrating improved capacity to maintain large-scale connectivity

**Table 8**  
Threshold levels setting.

Serial number	The value range of $\theta_i$	Node $V_i$ 's anti-damage resilience				
		Weak	Relatively weak	Moderate	Strong	Very strong
1	$\theta_i \geq 2$	0.7	0.6	0.5	0.4	0.3
2	$1 \leq \theta_i < 2$	0.6	0.5	0.4	0.3	0.2
3	$0.5 \leq \theta_i < 1$	0.5	0.4	0.3	0.2	0.1
4	$0.2 \leq \theta_i < 0.5$	0.3	0.2	0.1	0	0
5	$\theta_i < 0.2$	0	0	0	0	0

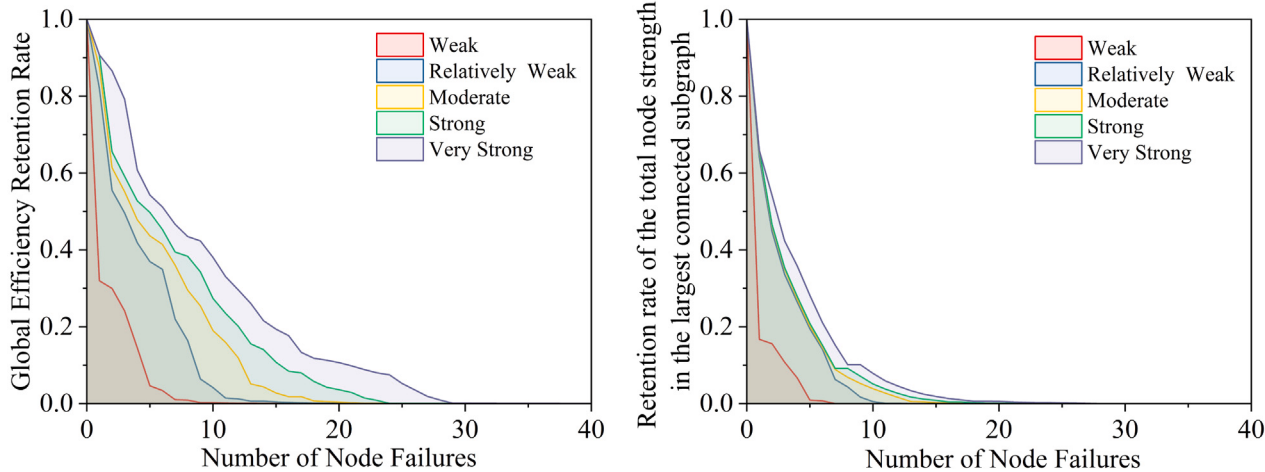


Fig. 11. Network performance retention rates at different failure coefficient levels in 2023.

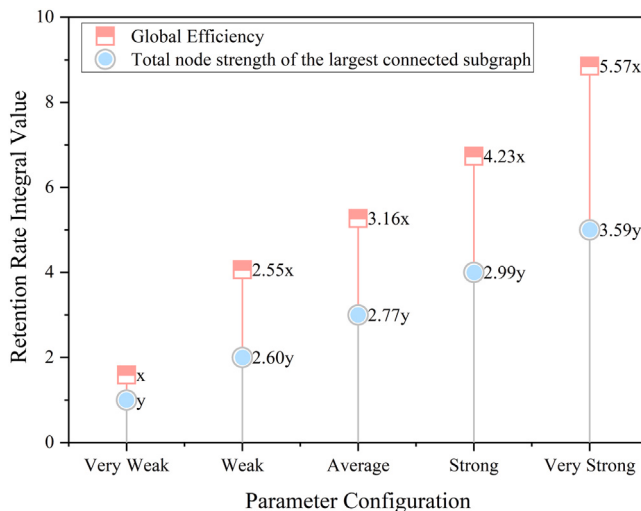


Fig. 12. Comparison of network resilience at different anti-destruction coefficient levels in 2023.

after damage. In the face of geopolitical risks and rising trade protectionism, measures taken by countries for resource security — such as increasing strategic reserves of wood pulp, diversifying import sources, and boosting domestic production capacity — can effectively reduce the failure threshold and enhance network resilience. Future research should focus on actual inventory strategies of different countries and the analysis of regional supply chain emergency protocols to further validate the relationship between theoretical parameters and real-world policies.

#### 4. Conclusions and discussion

This study constructs a directed weighted network model based on global pulp trade data from 2002 to 2023 and develops an underload cascading failure model to systematically evaluate the resilience of the global pulp trade network. Simulation results reveal:

(1) The global pulp trade network exhibits significant spatiotemporal evolution characteristics. While the number of nodes has decreased, the number of edges continues to grow, reinforcing the dominance of trade hubs. Core countries such as China and Brazil increasingly dominate the network, with a multipolar trend leading to the formation of five major communities. Although trade volume steadily increases, reflecting the industrial necessity of pulp, different external shocks demonstrate distinct impact patterns: the 2008 financial crisis triggered delayed effects through market adjustments, whereas the outbreak of the pandemic initiated immediate institutional interventions.

(2) Static resilience analysis shows a marked improvement in network transmission efficiency, although high-trade-volume countries are becoming less clustered. The assortativity pattern suggests continued dependency of smaller countries on central nodes, while power-law fitting indicates weakened hierarchical structures, suggesting that the diversified architecture enhances robustness against targeted attacks. Dynamic node resilience reveals China's leapfrog development as a hub node, with its incoming strength increasing by 5.14 times and weighted betweenness centrality rising by 3.54 times. In contrast, despite Brazil's strengthened export dominance, its global influence remains relatively limited.

(3) Cascading failure simulations show that the failure of critical nodes, such as Brazil, can trigger large-scale chain reactions, directly causing trade declines in 32 countries. Geospatial analysis highlights the most affected regions—Asia, the Americas, and Europe. Under targeted attack strategies, network performance loss far exceeds that under random disruptions, confirming the structural risks associated with

supply concentration. Dynamic resilience optimization indicates that reducing failure thresholds can enhance global efficiency redundancy by 5.57 times and increase the maximum connected subgraph strength by 3.59 times, offering quantitative support for resilience-enhancing strategies.

(4) External shocks have temporally differentiated impacts on network resilience. The 2008 financial crisis induced gradual network adaptation via market mechanisms in 2009, whereas the 2020 pandemic triggered immediate functional improvements, reflecting a “supply-priority” emergency response. This distinction not only validates Woods’ theory of crisis propagation but also reveals fundamental differences in how economic crises and public emergencies affect trade network resilience.

The key innovations of this study include:

(1) The first application of an underload cascading failure model to assess the resilience of pulp trade networks, breaking through the limitations of traditional static analyses. By simulating the failure scenarios of core exporting nations such as Brazil and Canada, this approach quantitatively uncovers cross-regional cascading paths, offering a novel methodology for risk early warning in supply chain disruptions.

(2) The development of a dynamic resilience assessment framework integrated with the underload cascading failure model, enabling end-to-end analysis from failure simulation to resilience quantification. Using cumulative integration methods, time-series responses are transformed into quantifiable metrics, addressing the lack of standardized resilience indicators in forest product trade networks.

(3) Spatiotemporal visualization captures the evolving influence of key nodes like China and Brazil, revealing the transition of the global pulp trade network from a dual-core structure to a multipolar system. Despite increased overall connectivity, regional dependence on dominant nodes still constitutes a potential systemic risk.

This study provides multidimensional scientific support for securing pulp supply chains and promoting sustainable management. Through static resilience analysis, countries can be classified as either hubs or peripheries within the network. Hub countries should focus on preventing supply chain fragmentation due to cascading failures, while peripheral countries should prioritize the establishment of diversified sourcing channels. Cascading failure simulations highlight vulnerabilities arising from supply dependencies, offering insights for countries to quantify import concentration indices and optimize regional trade partner selection. Dynamic resilience analysis also supports theoretical foundations for optimizing strategic reserve scales. Adjusting inventory thresholds dynamically according to geopolitical risk levels can alleviate supply–demand imbalances, avoid irrational procurement-induced overlogging, and promote sustainable forestry practices.

It is recommended that global forest certification systems incorporate import concentration assessments into audit criteria, requiring enterprises to initiate diversified sourcing when supply becomes overly concentrated to reduce deforestation risks. Regional trade agreements should include low-carbon logistics clauses to promote regionalized supply networks, shortening transportation distances and lowering carbon emissions. Meanwhile, multinational paper industry alliances can establish emergency collaboration mechanisms by sharing strategic reserves and production data, thereby minimizing restart losses caused by raw material shortages and jointly advancing clean production goals.

Future research will further explore the classification of OECD and Global South countries, analyzing how regional trade dependencies shape network resilience. By segmenting the world into geographic blocks, we aim to uncover regional resilience evolution patterns. Additionally, the coupling of geopolitical risks will help quantify their synergistic effects on sustainable forest management. The proposed methodology will be extended to other critical commodity networks such as timber and rare earths, establishing a multi-tiered resilience evaluation framework. This will provide theoretical support for countries to develop tailored resilience enhancement strategies aligned with their local network topologies.

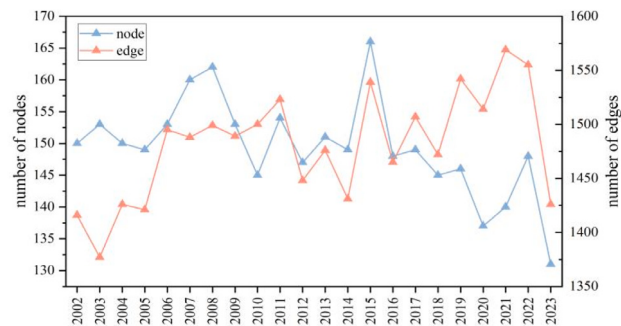


Fig. A.1. Temporal changes in the number of edges and nodes of the pulp trade from 2002 to 2023.

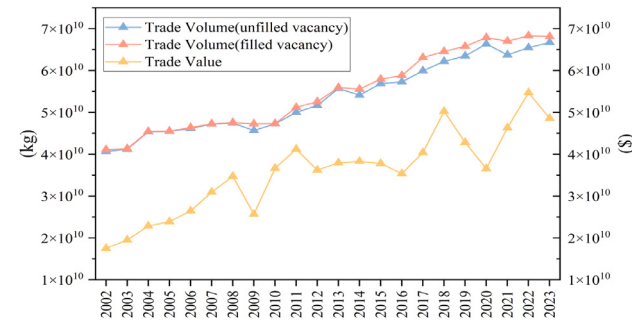


Fig. A.2. Temporal changes in the volume and value of global wood pulp trade network from 2002 to 2023.

## CRediT authorship contribution statement

**Wujun Tian:** Writing – review & editing, Writing – original draft, Visualization, Validation, Supervision, Software, Methodology, Investigation, Formal analysis, Data curation. **Xiangyu Huang:** Writing – review & editing, Writing – original draft, Validation, Supervision, Software, Resources, Methodology, Investigation, Formal analysis, Data curation, Conceptualization. **Liuguo Shao:** Validation, Resources, Methodology, Funding acquisition, Conceptualization. **Zhongwei Wang:** Resources, Methodology, Conceptualization. **Yihua Li:** Validation, Resources, Methodology, Investigation, Formal analysis.

## Declaration of competing interest

The authors declare that they have no known competing financial interests or personal relationships that could have appeared to influence the work reported in this paper.

## Acknowledgments

This research was supported by the Major Program of the National Social Science Fund of China (22&ZD098), National Science and Technology Major Project (2024ZD1002002), the Hunan Provincial Key Research and Development Program Project (2022GK2025), and the Hunan Provincial Key Laboratory of Intelligent Logistics Technology (2019TP1015).

## Appendix A

See Figs. A.1–A.8.

## Appendix B

See Table B.1.

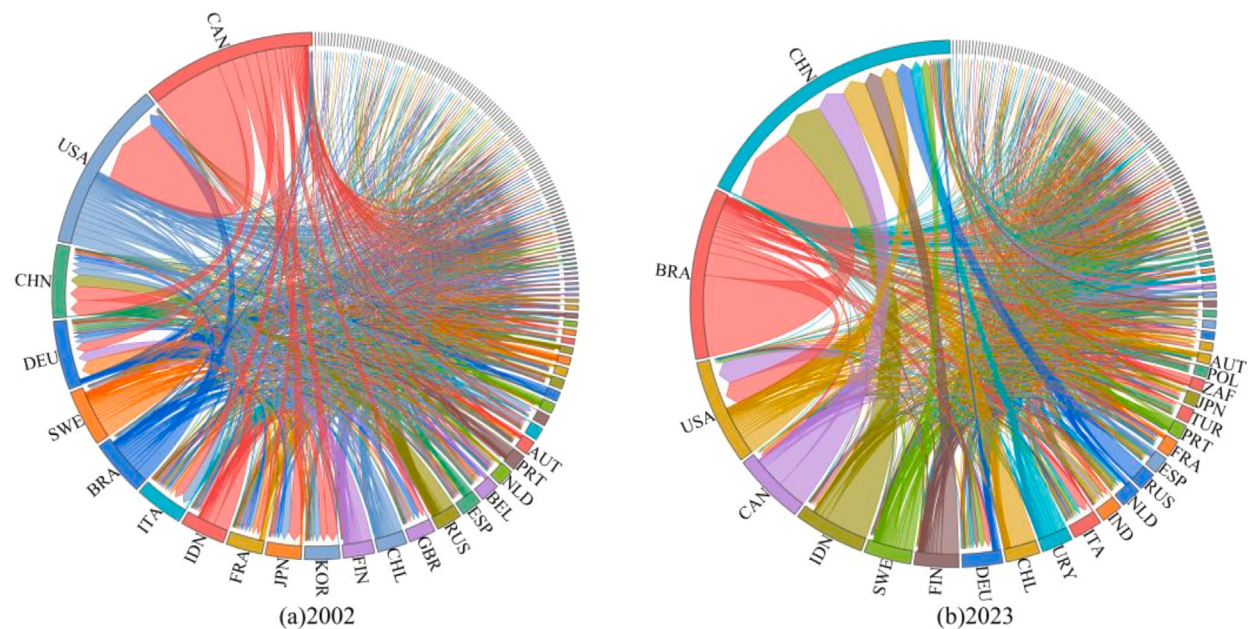


**Fig. A.3.** Topological structure of global wood pulp trade network in 2002 and 2023.

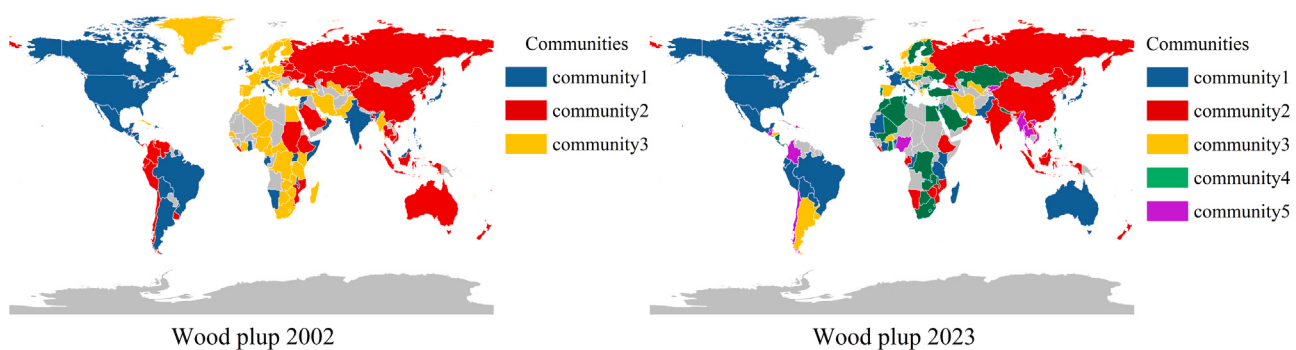


**Fig. A.4.** Geographic distribution of global wood pulp trade groups in 2002 and 2023.

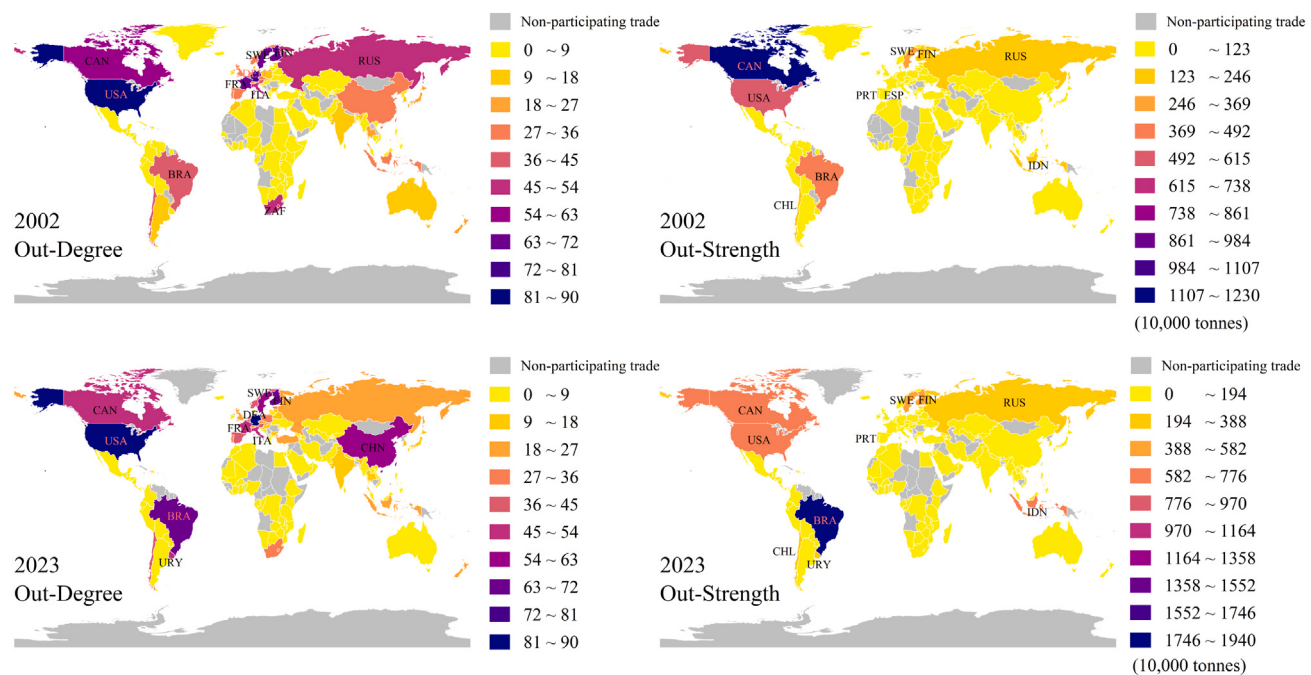


Fig. A.5. Network node out-degree and out-strength classification map (2002 & 2023).

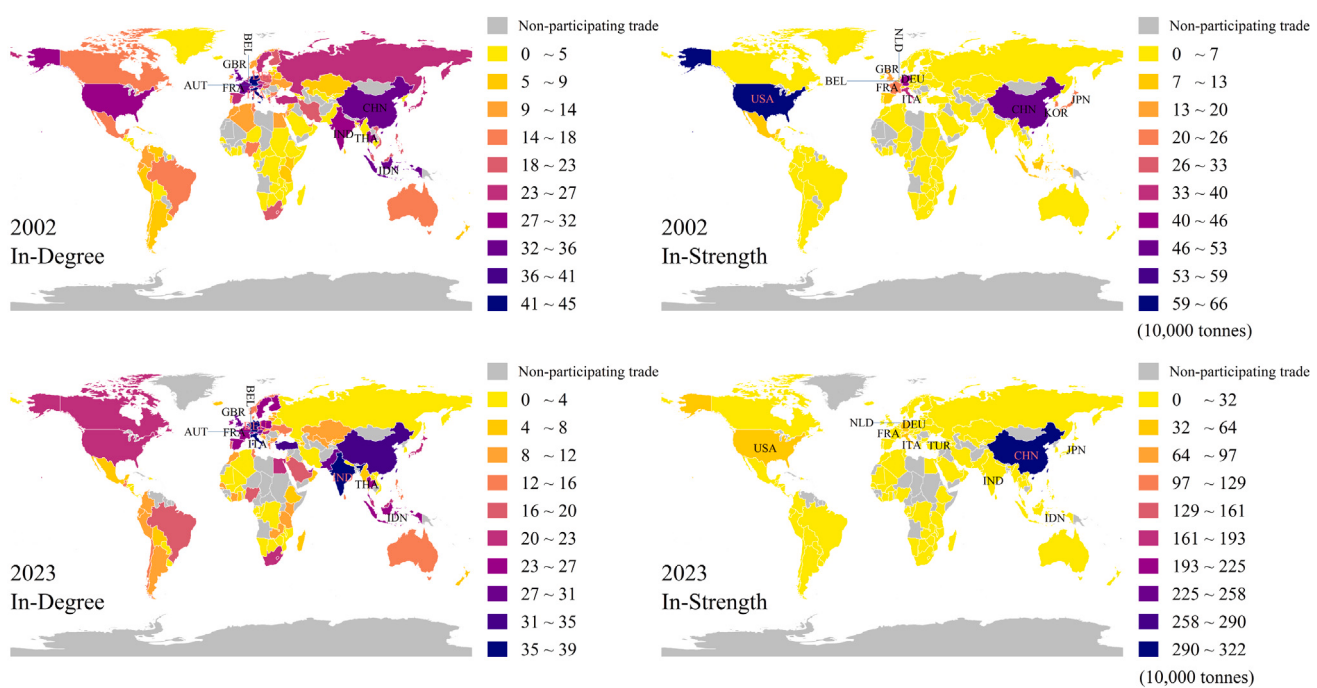
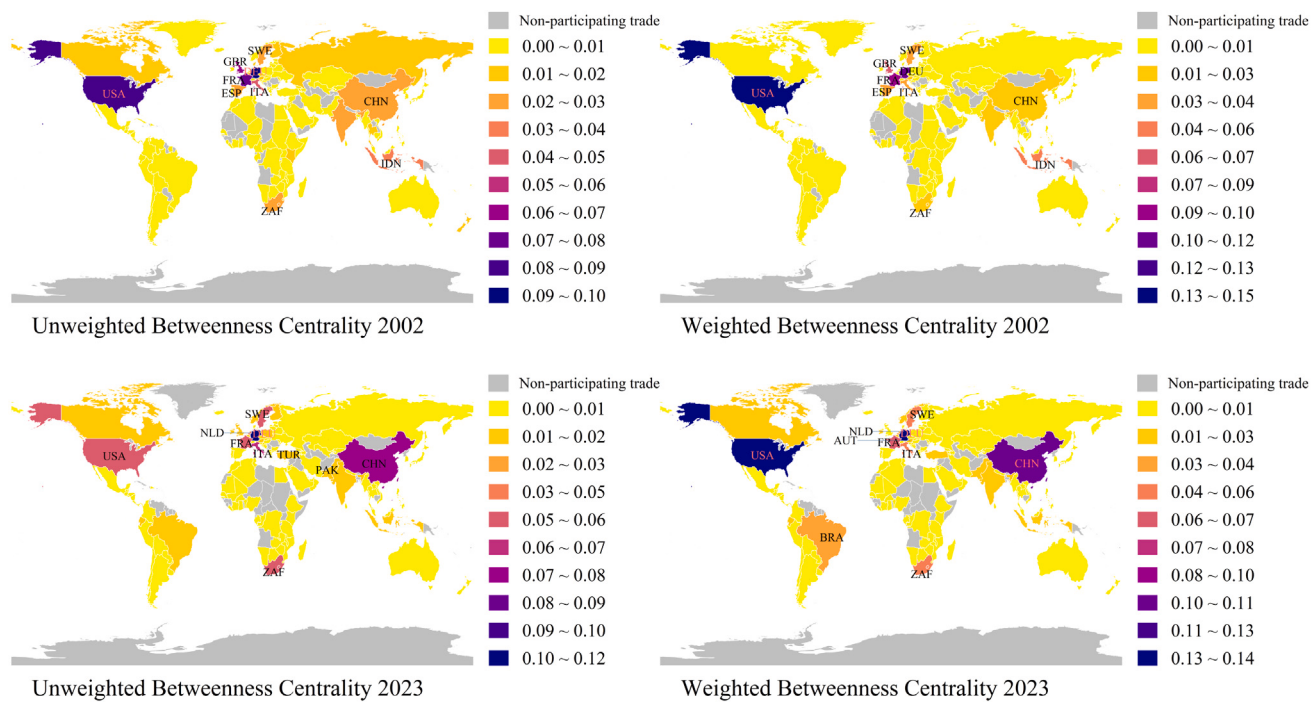
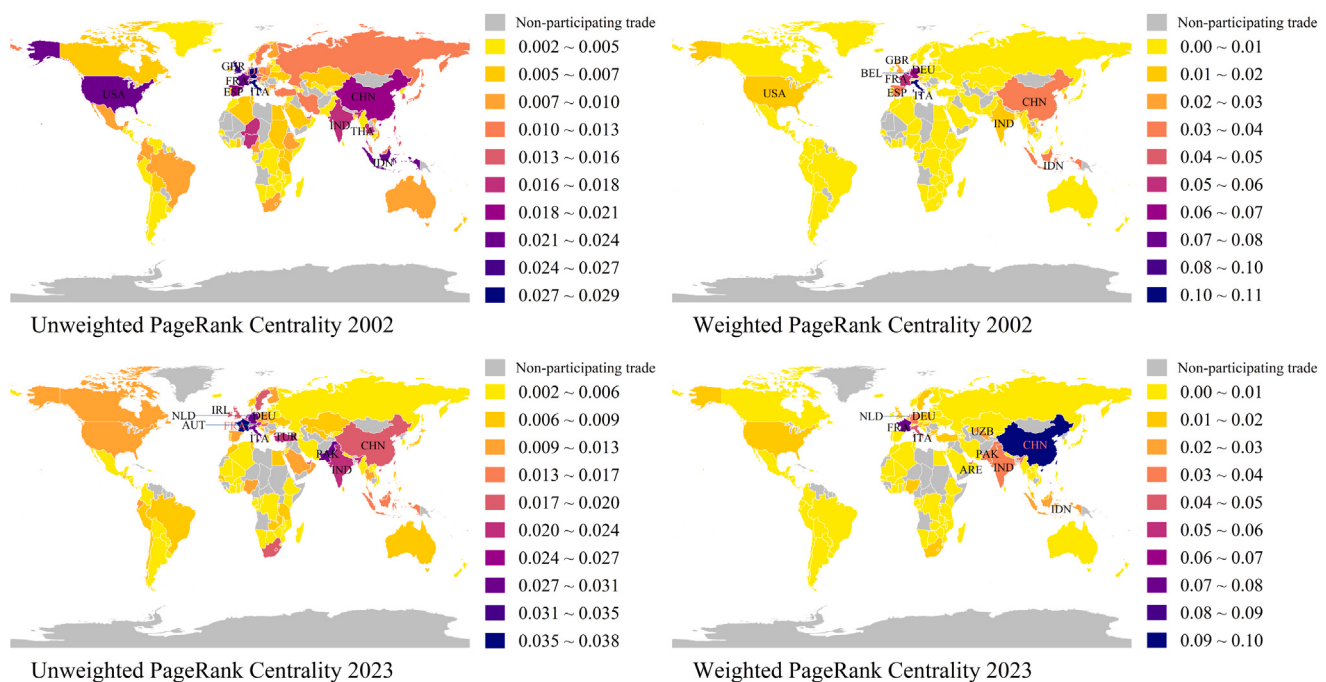


Fig. A.6. Network node in-degree and in-strength classification map (2002 & 2023).



**Fig. A.7.** Network node betweenness centrality classification map (2002 & 2023).



**Fig. A.8.** Network node PageRank centrality classification map (2002 & 2023).

**Table B.1**

Optimized Cascade Failure model pseudocode.

## Optimized Cascade Failure (OCF) Algorithm Specification

**Input:**

$G = (V, E)$ : Weighted directed graph  
 $start\_node$ : Initial failure node identifier  
Control parameters

**Output:**Modified network state  $G$  after cascade failure**Begin:****For each** node  $v \in V$ : //Initialization Phase

Set  $v.state \leftarrow \text{'normal'}$ ,  $v.round \leftarrow -1$  //Setting the initial state of a node  
 $v.load \leftarrow (\text{Eq. (8)})$  //Calculate intensity  
 $v.capacity \leftarrow v.load$  //Set Initial loads  
 $v.importance \leftarrow (\text{Eq. (18)})$  //Compute the importance of the node

**End for**Set  $start\_node.state \leftarrow \text{'lose'}$  //Trigger initial failure $start\_node.load \leftarrow 0$ **While** there exists  $new\_infected \neq \emptyset$ : //Cascade Propagation**For each** node  $v \in V$ :Update  $v.load \leftarrow (\text{Eq. (8)})$ 

State transition rules according to (Eq. (14))

**If**  $v.state = \text{'infected'}$ :Sort edges by  $importance$ , allocate  $\Delta w$  accordingly (Eq. (19)) // $\Delta w$  is the amount of export that needs to be reduced due to loads(Eq. (21))Compute  $\Delta w$  according to (Eq. (20)) //Residual distribution**If**  $v.state = \text{'lose'}$ :Set  $w(v, s) \leftarrow 0$ ,  $\forall s \in \text{successors}(v)$ **End for****End****Data availability**

The data presented in this study are available in UN Comtrade Database at <https://comtradeplus.un.org>, reference number is as shown in Table 3.

**References**

- Akbarzadeh, M., Memarmontazerin, S., Derrible, S., Reihani, S.F.S., 2019. The role of travel demand and network centrality on the connectivity and resilience of an urban street system. *Transportation* 46 (4), 1127–1141, <https://doi.org/10.1007/s11116-017-9814-y>.
- Andersson, E., Thollander, P., 2019. Key performance indicators for energy management in the Swedish pulp and paper industry. *Energy Strat. Rev.* 24, 229–235, <https://doi.org/10.1016/j.esr.2019.03.004>.
- Artimo, O., Grassia, M., De Domenico, M., Gleeson, J.P., Makse, H.A., Mangioni, G., Perc, M., Radicchi, F., 2024. Robustness and resilience of complex networks. *Nat. Rev. Phys.* 6 (2), 114–131, <https://doi.org/10.1038/s42254-023-00676-y>.
- Ash, J., Newth, D., 2007. Optimizing complex networks for resilience against cascading failure. *Phys. A* 380, 673–683, <https://doi.org/10.1016/j.physa.2006.12.058>.
- Azadegan, A., Dooley, K.J., 2021. A typology of supply network resilience strategies: Complex collaborations in a complex world. *J. Supply Chain Manag.* <https://doi.org/10.1111/jscm.12256>.
- Bai, X.W., Ma, Z.J., Zhou, Y.M., 2023. Data-driven static and dynamic resilience assessment of the global liner shipping network. *Transp. Res. Part E- Logist. Transp. Res.* 170, 19, <https://doi.org/10.1016/j.tre.2023.103016>.
- Berche, B., von Ferber, C., Holovatch, T., Holovatch, Y., 2009. Resilience of public transport networks against attacks. *Eur. Phys. J. B* 71 (1), 125–137, <https://doi.org/10.1140/epjb/e2009-00291-3>.
- Cai, H.B., Song, Y.Y., 2016. The state's position in international agricultural commodity trade a complex network. *China Agric. Econ. Rev.* 8 (3), 430–442, <https://doi.org/10.1108/caer-02-2016-0032>.
- Carreras, B.A., Lynch, V.E., Dobson, I., Newman, D.E., 2002. Critical points and transitions in an electric power transmission model for cascading failure blackouts. *Chaos* 12 (4), 985–994, <https://doi.org/10.1063/1.1505810>.
- Chen, Y.R., Chen, M.P., 2023. Evolution of the global phosphorus trade network: A production perspective on resilience. *J. Clean. Prod.* 405, 10, <https://doi.org/10.1016/j.jclepro.2023.136843>.
- Chen, Z.H., Wang, H., Liu, X.Y., Wang, Z., Wen, S.B., 2022. Risk diffusion of international oil trade cuts: A network-based dynamics model. *Energy Rep.* 8, 11320–11333, <https://doi.org/10.1016/j.egyrep.2022.08.244>.
- Chopra, S.S., Dillon, T., Bilec, M.M., Khanna, V., 2016. A network-based framework for assessing infrastructure resilience: A case study of the London metro system. *J. R. Soc. Interface* 13 (118), 11, <https://doi.org/10.1098/rsif.2016.0113>.
- Clark, K.L., Bhatia, U., Kodra, E.A., Ganguly, A.R., 2018. Resilience of the US national airspace system airport network. *Ieee Trans. Intell. Transp. Syst.* 19 (12), 3785–3794, <https://doi.org/10.1109/tits.2017.2784391>.
- de Carvalho, K.H.A., da Silva, M.L., Soares, N.S., 2009. Competitiveness of Brazilian wood pulp in the international market. *Cerne* 15 (4), 383–390, <https://www.redalyc.org/pdf/744/74413024001.pdf>.
- Dong, G., Wang, F., Shekhtman, L.M., Danziger, M.M., Fan, J., Du, R., Liu, J., Tian, L., Stanley, H.E., Havlin, S., 2021. Optimal resilience of modular interacting networks. *Proc. Natl. Acad. Sci.* 118 (22), e1922831118, <https://doi.org/10.1073/pnas.1922831118>.
- Duan, D.-L., Ling, X.-D., Wu, X.-Y., OuYang, D.-H., Zhong, B., 2014. Critical thresholds for scale-free networks against cascading failures. *Phys. A* 416, 252–258, <https://doi.org/10.1016/j.physa.2014.08.040>.
- Duan, D.-L., Wu, J., Deng, H.Z., Sha, F., Tan, Y.J., 2013. Cascading failure model of complex networks based on tunable load redistribution. *Syst. Engineering- Theory & Pr.* 33 (1), 203–208.
- Duo, W.J.L., 2010. Cading failures on complex networks based on local characteristics of nodes. *J. Manag. Sci. Eng.* 13 (8), 9.
- Fang, W., Minghua, T., Runsheng, Y.I.N., Zhonghua, Y.I.N., Zhenyu, Z., 2021. Change of global woody forest products trading network and relationship between large supply and demand countries. *Resour. Sci.* 43 (5), 1008–1024, <https://doi.org/10.18402/resci.2021.05.14>.
- Gao, J.X., Barzel, B., Barabási, A.L., 2016. Universal resilience patterns in complex networks. *Nature* 530 (7590), 307–312, <https://doi.org/10.1038/nature16948>.
- Gao, J.X., Liu, X.M., Li, D.Q., Havlin, S., 2015a. Recent progress on the resilience of complex networks. *Energies* 8 (10), 12187–12210, <https://doi.org/10.3390/en81012187>.
- Gao, J., Liu, X., Li, D., Havlin, S., 2015b. Recent progress on the resilience of complex networks. *Energies* <https://doi.org/10.3390/en81012187>.
- Herrera, M., Abraham, E., Stoianov, I., 2016. A graph-theoretic framework for assessing the resilience of sectorised water distribution networks. *Water Resour. Manag.* 30 (5), 1685–1699, <https://doi.org/10.1007/s11269-016-1245-6>.
- Holling, C.S., 1973. Resilience and stability of ecological systems. *Annu. Rev. Ecol. Evol. Syst.* 4, 1–23, <https://doi.org/10.1017/9781009177856.038>.
- Holme, P., Kim, B.J., Yoon, C.N., Han, S.K., 2002. Attack vulnerability of complex networks. *Phys. Rev. E* 65 (5), 056109, <https://doi.org/10.1103/PhysRevE.65.056109>.
- Huang, X., Wang, Z., Pang, Y., Tian, W., 2025. Evolution of disruption resilience in the wood forest products trade network, considering the propagation of disruption risks and underload cascading failure. *Sustainability* 17 (6), <https://doi.org/10.3390/su17062733>.
- Huang, X., Wang, Z., Pang, Y., Tian, W., Zhang, M., 2024. Static resilience evolution of the global wood forest products trade network: A complex directed weighted network analysis. *Forests* <https://doi.org/10.3390/f15091665>.
- Hujala, M., Arminen, H., Hill, R.C., Puusalainen, K., 2013. Explaining the shifts of international trade in pulp and paper industry. *For. Sci.* 59 (2), 211–222, <https://doi.org/10.5849/forsci.11-078>.

- Ji, G., Zhong, H., Feukam Nzudie, H.L., Wang, P., Tian, P., 2024a. The structure, dynamics, and vulnerability of the global food trade network. *J. Clean. Prod.* 434, 140439, <https://doi.org/10.1016/j.jclepro.2023.140439>.
- Ji, G., Zhong, H., Nzudie, H.L.F., Wang, P., Tian, P., 2024b. The structure, dynamics, and vulnerability of the global food trade network. *J. Clean. Prod.* (Jan.1), 434, <https://doi.org/10.1016/j.jclepro.2023.140439>.
- John, A., Yang, Z.L., Riahi, R., Wang, J., 2016. A risk assessment approach to improve the resilience of a seaport system using Bayesian networks. *Ocean Eng.* 111, 136–147, <https://doi.org/10.1016/j.oceaneng.2015.10.048>.
- Kammouh, O., Gardoni, P., Cimellaro, G.P., 2020. Probabilistic framework to evaluate the resilience of engineering systems using Bayesian and dynamic Bayesian networks. *Reliab. Eng. Syst. Saf.* 198, 20, <https://doi.org/10.1016/j.ress.2020.106813>.
- Kharrazi, A., Akiyama, T., Yu, Y.D., Li, J., 2016. Evaluating the evolution of the hehei river basin using the ecological network analysis: Efficiency, resilience, and implications for water resource management policy. *Sci. Total Environ.* 572, 688–696, <https://doi.org/10.1016/j.scitotenv.2016.06.210>.
- Kharrazi, A., Rovenskaya, E., Fath, B.D., 2017. Network structure impacts global commodity trade growth and resilience. *Plos One* 12 (2), 13, <https://doi.org/10.1371/journal.pone.0171184>.
- Kilanitis, I., Sextos, A., 2019. Integrated seismic risk and resilience assessment of roadway networks in earthquake prone areas. *Bull. Earthq. Eng.* 17 (1), 181–210, <https://doi.org/10.1007/s10518-018-0457-y>.
- Kim, Y., Chen, Y.S., Linderman, K., 2015. Supply network disruption and resilience: A network structural perspective. *J. Oper. Manage.* 33–34, 43–59, <https://doi.org/10.1016/j.jom.2014.10.006>.
- Kim, D.H., Eisenberg, D.A., Chun, Y.H., Park, J., 2017. Network topology and resilience analysis of South Korean power grid. *Phys. A- Stat. Mech. Appl.* 465, 13–24, <https://doi.org/10.1016/j.physa.2016.08.002>.
- Lee, K.M., Goh, K.I., 2016. Strength of weak layers in cascading failures on multiplex networks: Case of the international trade network. *Sci. Rep.* 6, 9, <https://doi.org/10.1038/srep26346>.
- Lee, D.S., Goh, K.I., Kahng, B., Kim, D., 2004. Sandpile avalanche dynamics on scale-free networks. *Phys. A Stat. Mech. Appl.* 338 (1), 84–91, <https://doi.org/10.1016/j.physa.2004.02.028>.
- Li, J., Nie, W., Zhang, M., Wang, L., Dong, H., Xu, B., 2024. Assessment and optimization of urban ecological network resilience based on disturbance scenario simulations: A case study of nanjing city. *J. Clean. Prod.* 438, 140812, <https://doi.org/10.1016/j.jclepro.2024.140812>.
- Li, P., Wang, B.H., Sun, H., Gao, P., Zhou, T., 2008. A limited resource model of fault-tolerant capability against cascading failure of complex network. *Eur. Phys. J. B* 62 (1), 101–104, <https://doi.org/10.1140/epjb/e2008-00114-1>.
- Li, L., Zhang, P., Tan, J., Guan, H., 2019. Review on the evolution of resilience concept and research progress on regional economic resilience. *Hum. Geogr.* 34, 1–7.
- Li, Y.H., Zobel, C.W., Seref, O., Chatfield, D., 2020a. Network characteristics and supply chain resilience under conditions of risk propagation. *Int. J. Prod. Econ.* 223, 13, <https://doi.org/10.1016/j.ijpe.2019.107529>.
- Li, Y., Zobel, C.W., Seref, O., Chatfield, D., 2020b. Network characteristics and supply chain resilience under conditions of risk propagation. *Int. J. Prod. Econ.* 223, <https://doi.org/10.1016/j.ijpe.2019.107529>.
- Liu, L., Chen, Y., Yu, J., Cheng, R., 2024. Analysis of the trade network of global wood forest products and its evolution from 1995 to 2020. *For. Prod. J.* 74 (2), 121–129, <https://doi.org/10.13073/fpj-d-23-00065>.
- Liu, X.M., Li, D.Q., Ma, M.Q., Szymanski, B.K., Stanley, H.E., Gao, J.X., 2022. Network resilience. *Phys. Reports- Rev. Sect. Phys. Lett.* 971, 1–108, <https://doi.org/10.1016/j.physrep.2022.04.002>.
- Liu, W., Song, Z.Y., 2020. Review of studies on the resilience of urban critical infrastructure networks. *Reliab. Eng. Syst. Saf.* 193, 16, <https://doi.org/10.1016/j.ress.2019.106617>.
- Liu, K., Wang, H., Liu, H.Y., Nie, S.X., Du, H.S., Si, C.L., 2020. COVID-19: Challenges and perspectives for the pulp and paper industry worldwide. *Bioresources* 15 (3), 4638–4641, <https://bioresources.cnr.ncsu.edu/resources/covid-19-challenges-and-perspectives-for-the-pulp-and-paper-industry-worldwide>.
- Lovric, M., De Re, R., Vidale, E., Pettenella, D., Mavsar, R., 2018. Social network analysis as a tool for the analysis of international trade of wood and non-wood forest products. *For. Policy Econ.* 86, 45–66, <https://doi.org/10.1016/j.fopol.2017.10.006>.
- McCarthy, P., Lei, L., 2010. Regional demands for pulp and paper products. *J. For. Econ.* 16 (2), 127–144, <https://doi.org/10.1016/j.jfe.2009.11.001>.
- Meng, Y.Y., Zhao, X.F., Liu, J.Z., Qi, Q.J., 2023. Dynamic influence analysis of the important station evolution on the resilience of complex metro network. *Sustainability* 15 (12), 15, <https://doi.org/10.3390/su15129309>.
- Miao, C.H., Wan, Y.F., Kang, M.L., Xiang, F., 2024. Topological analysis, endogenous mechanisms, and supply risk propagation in the polycrystalline silicon trade dependency network. *J. Clean. Prod.* 439, 18, <https://doi.org/10.1016/j.jclepro.2024.140657>.
- Mohammed, A., Govindan, K., Zubairu, N., Pratabaraj, J., Abideen, A.Z., 2023. Multi-tier supply chain network design: A key towards sustainability and resilience. *Comput. Ind. Eng.* 182, 18, <https://doi.org/10.1016/j.cie.2023.109396>.
- Moreno, Y., Gómez, J.B., Pacheco, A.F., 2001. Instability of scale-free networks under node-breaking avalanches. *EPL (Eur. Letters)* 58 (4), 630. <http://dx.doi.org/10.1209/epl/i2002-00442-2>.
- Moreno, Y., Pastor-Satorras, R., Vázquez, A., Vespignani, A., 2007. Critical load and congestion instabilities in scale-free networks. *Europhys. Lett.* 62 (2), 292. <http://dx.doi.org/10.1209/epl/i2003-00140-7>.
- Reggiani, A., 2013. Network resilience for transport security: Some methodological considerations. *Transp. Policy* 28, 63–68, <https://doi.org/10.1016/j.tranpol.2012.09.007>.
- Rossato, F., Susaeta, A., Adams, D.C., Hidalgo, I.G., de Araujo, T.D., de Queiroz, A., 2018. Comparison of revealed comparative advantage indexes with application to trade tendencies of cellulose production from planted forests in Brazil, Canada, China, Sweden, Finland and the United States. *For. Policy Econ.* 97, 59–66, <https://doi.org/10.1016/j.fopol.2018.09.007>.
- Sansavini, G., Hajj, M.R., Puri, I.K., Zio, E., 2009. A deterministic representation of cascade spreading in complex networks. *Epl* 87 (4), 48004, <https://doi.org/10.1209-0295-5075/87/48004>.
- Serre, D., Heinzel, C., 2018. Assessing and mapping urban resilience to floods with respect to cascading effects through critical infrastructure networks. *Int. J. Disaster Risk Reduct.* 30, 235–243, <https://doi.org/10.1016/j.ijdrr.2018.02.018>.
- Sun, C.Y., 2015. An investigation of China's import demand for wood pulp and wastepaper. *For. Policy Econ.* 61, 113–121, <https://doi.org/10.1016/j.fopol.2015.10.001>.
- Sun, X.Q., Shi, Q., Hao, X.Q., 2022. Supply crisis propagation in the global cobalt trade network. *Resour. Conserv. Recycl.* 179, 10, <https://doi.org/10.1016/j.resconrec.2021.106035>.
- Sun, X., Wei, Y., Jin, Y., Song, W., Li, X., 2023. The evolution of structural resilience of global oil and gas resources trade network. *Glob. Networks* 23 (2), 391–411, <https://doi.org/10.1111/glob.12399>.
- Wan, Z.L., Mahajan, Y., Kang, B.W., Moore, T.J., Cho, J.H., 2021a. A survey on centrality metrics and their network resilience analysis. *Ieee Access* 9, 104773–104819, <https://doi.org/10.1109/access.2021.3094196>.
- Wan, Z., Mahajan, Y., Kang, B.W., Moore, T.J., Cho, J.H., 2021b. A survey on centrality metrics and their network resilience analysis. *IEEE Access PP* (99), 1–1. <https://doi.org/10.1109/ACCESS.2021.3094196>.
- Wang, Y., Chen, L., Wang, X.Y., Tang, N., Kang, X.Y., 2023a. Trade network characteristics, competitive patterns, and potential risk shock propagation in global aluminum ore trade. *Front. Energy Res.* 10, 15, <https://doi.org/10.3389/fenrg.2022.104816>.
- Wang, J.-S., Wu, X.-P., Chen, Y.-Q., 2013. Invulnerability of weighted scale free networks against cascading failure. *Complex Syst. Complex. Sci.* 10 (2), 13–19.
- Wang, R., Wu, H.M., Zhe, R., Zhang, Y.A., 2023b. Complex network analysis of global forest products trade pattern. *Can. J. Forest Res.* 53 (4), 271–283, <https://doi.org/10.1139/cjfr-2022-0286>.
- Wei, Y., Xiu, C., 2020. Study on the concept and analytical framework of city network resilience. *Prog. Geogr.* 39 (3), 488–502.
- Woods, N., 2014. *The Globalizers: the IMF, The World Bank, and Their Borrowers*. Cornell University Press.
- Worku, L.A., Bachheti, A., Bachheti, R.K., Reis, C.R., Chandel, A.K., 2023. Agricultural residues as raw materials for pulp and paper production: Overview and applications on membrane fabrication. *Membranes* 13 (2), 17, <https://doi.org/10.3390/membranes13020228>.
- World Bank, 2024. Imports, exports, and mirror data. [https://wits.worldbank.org/wits/witshelp/content/data\\_retrieval/T/Intro/B2.Imports\\_Exports\\_and\\_Mirror.htm](https://wits.worldbank.org/wits/witshelp/content/data_retrieval/T/Intro/B2.Imports_Exports_and_Mirror.htm). (Accessed 28 April 2025).
- Wu, Z., Cheng, S., Xu, K., Qian, Y., 2024. Ecological network resilience evaluation and ecological strategic space identification based on complex network theory: A case study of nanjing city. *Ecol. Indic.* 158, 111604, <https://doi.org/10.1016/j.ecolind.2024.111604>.
- Xia, Y., Fan, J., Hill, D., 2010. Cascading failure in Watts-Strogatz small-world networks. *Phys. A* 389 (6), 1281–1285, <https://doi.org/10.1016/j.physa.2009.11.037>.
- Xiang, Q., Yu, H., Huang, H., Li, F., Ju, L.F., Hu, W., Yu, P., Deng, Z.C., Chen, Y.N., 2024. Assessing the resilience of complex ecological spatial networks using a cascading failure model. *J. Clean. Prod.* 434 (Jan.1), 434, <https://doi.org/10.1016/j.jclepro.2023.140014>.
- Xu, C., Xu, X.G., 2024. A two-stage resilience promotion approach for urban rail transit networks based on topology enhancement and recovery optimization. *Phys. A- Stat. Mech. Appl.* 635, 28, <https://doi.org/10.1016/j.physa.2024.129496>.
- Yuan, X.J., Ge, C.B., Liu, Y.P., Li, N., Wang, Y., 2022. Evolution of global crude oil trade network structure and resilience. *Sustainability* 14 (23), 21, <https://doi.org/10.3390/su142316059>.
- Zhao, K., Kumar, A., Harrison, T.P., Yen, J., 2011. Analyzing the resilience of complex supply network topologies against random and targeted disruptions. *Ieee Syst. J.* 5 (1), 28–39, <https://doi.org/10.1109/jsyst.2010.2100192>.

Zhao, L.F., Yang, Y.J., Bai, X., Chen, L., Lu, A.L., Zhang, X., Chen, W.Q., 2023. Structure, robustness and supply risk in the global wind turbine trade network. *Renew. Sustain. Energy Rev.* 177, 18, <https://doi.org/10.1016/j.rser.2023.113214>.

Zhou, Y.Y., Hong, Y.P., Cheng, B.D., Xiong, L.C., 2021. The spatial correlation and driving mechanism of wood-based products trade network in RCEP countries. *Sustainability* 13 (18), 16, <https://doi.org/10.3390/su131810063>.